JOURNAL OF GEOPHYSICAL RESEARCH, VOL. 97, NO. D15, PAGES 16,395–16,419, OCTOBER 30, 1992

Meteorological Overview of the Arctic Boundary Layer Expedition (ABLE 3A) Flight Series

MARK C. SHIPHAM

Atmospheric Sciences Division, NASA Langley Research Center, Hampton, Virginia

A. SCOTT BACHMEIER

Lockheed Engineering and Sciences Company, Hampton, Virginia

DONALD R. CAHOON, JR., AND EDWARD V. BROWELL

Atmospheric Sciences Division, NASA Langley Research Center, Hampton, Virginia

A meteorological overview of the Arctic Boundary Layer Expedition (ABLE 3A) flight series is presented. Synoptic analyses of mid-tropospheric circulation patterns are combined with isentropic back trajectory calculations to describe the long-range (400–3000 km) atmospheric transport mechanisms and pathways of air masses to the Arctic and sub-Arctic regions of North America during July and August 1988. Siberia and the northern Pacific Ocean were found to be the two most likely source areas for 3-day transport to the study areas in Alaska. Transport to the Barrow region was frequently influenced by polar vortices and associated short-wave troughs over the Arctic Ocean, while the Bethel area was most often affected by lows migrating across the Bering Sea and the Gulf of Alaska, as well as ridges of high pressure which built into interior Alaska. July 1988 was warmer and dryer than normal over much of Alaska. As a result, the 1988 Alaska fire season was one of the most active of the past decade. Airborne lidar measurements verified the presence of biomass burning plumes on many flights, often trapped in thin subsidence layer temperature inversions. Several cases of stratosphere/troposphere exchange were noted, based upon potential vorticity analyses and aircraft lidar data, especially in the Barrow region and during transit flights to and from Alaska.

INTRODUCTION

During July and August 1988, the Arctic Boundary Layer Expedition (ABLE 3A) was conducted in Arctic and sub-Arctic regions of North America (see *Harriss et al.* [this issue] for an overview). Thirty-three aircraft missions were carried out in an effort to characterize the mid-tropospheric distributions and variability of trace gas and aerosol species, and to investigate the role of long-range atmospheric transport of pollutants into the study regions.

Beginning in the late 1940s and early 1950s, episodes of widespread wintertime Arctic haze were observed by weather reconnaissance aircraft over Alaska. Subsequent research during the past two decades has established that this haze is caused by the long-range transport of mid-latitude pollution into the Arctic troposphere during winter and early spring [*Barrie et al.*, 1981; *Rahn*, 1981; *Schnell*, 1984]. In discussing the winter Arctic haze phenomenon, Barrie described the Arctic atmosphere using a "bathtub model," the Arctic atmosphere being a horizontally mixed reservoir into which air from mid-latitudes is periodically injected from the south. These injections normally lasted from 1 to 3 days and originated in the heavily industrialized regions between 30°N and 60°N latitude (eastern North America/Japan-China/Europe/northern Asia). However, the normal summer transport regime does not link the Arctic with the mid-latitudes as well as in winter, and more efficient pollutant scavenging processes (greater cloud cover and precipitation) tend to clean the summertime air masses before they reach the Arctic. In addition, the summer Arctic atmosphere experiences less stagnation and more turbulent mixing than in winter, creating a far less favorable environment for the formation of thick haze layers.

In this paper, we have chosen to follow the approach of *Raatz* [1984], combining synoptic analyses of mid-tropospheric circulation patterns with isentropic back trajectory calculations to describe the transport mechanisms and pathways of air masses to the ABLE 3A study areas. Our findings for the summer of 1988 indicate that Siberia and the northern Pacific were the two most likely source areas for long-range (400–3000 km) transport to the Alaska region. This is in general agreement with *Miller* [1981], who also concluded that the northern Pacific and Asia/Europe were the two source areas of long-range (>2000 km) transport to Barrow, Alaska. It is therefore evident that the Alaskan Arctic is subject to inputs from both maritime (oceanic) and continental air masses.

ATMOSPHERIC TRANSPORT TO THE ARCTIC: AIR MASSES AND TRAJECTORY ANALYSIS

Two air mass source regions are important when considering summertime meteorological transport to Alaska: the "primary" source region of interior Siberia and the "secondary" source region of the northern Pacific Ocean between the Soviet Union and Canada [*Taylor*, 1954]. Primary source regions are characterized by a uniformity of surface along with the frequent stagnation of air, during which the air

Paper number 91JD02640.
0148-0227/92/91JD-02640$05.00

can arrive at equilibrium with the surface (via convective mixing) in 2–4 days. Secondary source regions also have an extensive uniform surface, but the airflow is usually not stagnant; if air passing over such a region can be modified rapidly enough, it may take on unique characteristics that justify labeling it a distinct air mass. For a relatively cold surface such as the northern Pacific Ocean in summer, the overlying air often becomes stable with little vertical mixing, and equilibrium with the water surface may take 1–2 weeks. The Arctic Ocean icepack may also be considered a secondary source region for summertime transport to Alaska, when a northerly flow reaches the Barrow region and the northern slopes of the Brooks Range.

The concepts of air mass types and air mass source regions can be readily applied when referring to the lower troposphere, namely, the planetary boundary layer (corresponding roughly to the lowest 1 km). In the free troposphere above the planetary boundary layer, air mass classification and the impact of primary and secondary source regions become more difficult to define. Following the air mass classifications developed by *Bergeron* [1928], Alaskan air transported from Siberia or other parts of the Asian continent will be termed continental polar (cP). If the cP air mass spends enough time over the Bering Sea, northern Pacific, or the Gulf of Alaska, it can take on properties resembling maritime polar (mP) air. In this paper, we will refer to these modified air masses as mP, although they are essentially cP with a maritime influence. In fact, *Gregory et al.* [this issue] found little difference in the ozone and fine aerosol number-density composition when comparing "cP air masses" with "mP air masses" transported to Alaska. Aerosol sizing data, however, suggested that the cP air masses were modified by marine components at the lower altitudes (<5 km). Even though air mass classification has fallen out of favor in modern synoptic meteorology, it does serve here as a convenient method for helping to separate air chemistry signatures observed during ABLE 3A.

An isentropic trajectory technique originally developed by *Danielsen* [1961, 1966] and further refined by *Haagensen and Shapiro* [1979] was utilized to compute trajectories for this paper. Most of the backward trajectory analyses are for a 72-hour time period unless otherwise noted, which closely represents the expected lifetime of many pollutants in arctic regions during the summer months [*Gregory et al.*, this issue]. The potential temperature (theta) surfaces chosen for the figures in this paper are those most representative of the predominant aircraft altitudes during each flight. Other output products from the trajectory package include objective analyses of potential vorticity, which are used to identify regions where stratospheric air has been mixed downward into the middle and upper troposphere [*Hoskins et al.*, 1985; *Shapiro et al.*, 1987].

The trajectory package only approximates synoptic-scale flow due to theoretical restrictions in the model. The primary constraint of adiabatic flow is a poor assumption in regions of the atmosphere where diabatic processes such as latent heating/evaporative cooling, terrestrial/solar radiation, and sensible heat exchanges are large. However, such diabatic heating and cooling processes are usually secondary in importance for the time scales (1–5 days) considered here [*Moore*, 1987]. The limited availability of wind data over oceans and other remote areas also affects the accuracy of trajectories in such regions. Assessment of trajectory errors requires tracer verification techniques to be performed, and recent studies have shown that average horizontal position errors after 1 day of transport ranged from 180 to 290 km [*Harris and Kahl*, 1990]. Previous studies [*Borys and Rahn*, 1981; *Radke et al.*, 1984; *Kahl et al.*, 1989] support the use of trajectories to determine the general synoptic-scale airflow in Arctic regions.

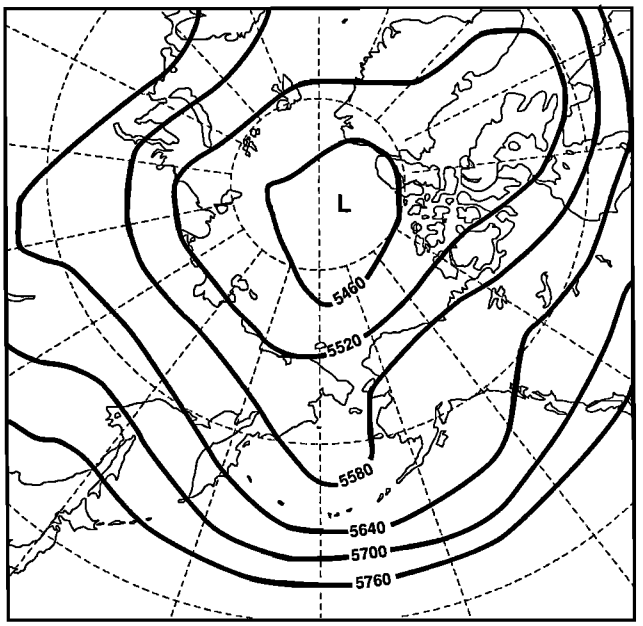

Fig. 1. Mean 500 hPa heights (in geopotential meters) for July–August 1988, derived from National Meteorological Center gridded data analyses (2.5° by 2.5° latitude/longitude grid).

SUMMER 1988 CLIMATIC SUMMARY

The mean height field at 500 hPa for July–August 1988 is shown in Figure 1. The location of the polar vortex was over the Arctic Ocean, with an associated trough of low pressure over the Bering Sea. This mid-tropospheric flow pattern was very representative of the climatological normal. However, the 500-hPa heights averaged for July 1988 (Figure 2) show a ridge of high pressure over interior Alaska, which was responsible for the warm and dry conditions observed during that month. July mean temperatures were 2.9°C (5.3°F) above normal at Bethel and 2.4°C (4.3°F) above normal at Fairbanks, while total precipitation for the month was 26% of the normal amount and 57% of the normal amount, respectively. In addition, a ridge of high pressure existed over eastern Asia. For August 1988 (Figure 3), the mean 500-hPa height field shows that the ridge had weakened over Alaska, and the trough over the Bering Sea had become the predominant feature as the long-wave flow pattern was tending to move back towards the climatological normal by the end of August.

Daily 500-hPa maps derived from National Meteorological Center gridded data analyses are displayed in Figures 4*a*–4*v* for each of the days when flight missions were conducted over Alaska. Centers of low (L) and high (H) pressure are annotated on the maps, as well as the axes of troughs (heavy dashed lines) and ridges (heavy jagged lines).

As a consequence of the warm and dry weather, one of the most active fire seasons of the past decade was observed.

Over 600 fires were reported, with more than 8500 km^2 (2.1 million acres) burned statewide [*Alaska Fire Service*, 1989]. Low relative humidities (frequently less than 30%) and unusually windy conditions (4.5–9.0 m s^{-1}, 10–20 mph) during the month of July caused many of the fires to increase rapidly in size. A large amount of smoke was generated, which began to fill the large shallow basins of interior Alaska. The resulting visibility problems due to smoke caused major safety concerns for aviation, and some air space closures were necessary over the Yukon Flats region. The majority of the fires were found in the 65°N to 67°N latitude belt across the interior of Alaska (the Yukon River Valley), including the six fires larger than 405 km^2 (100,000 acres) (Table 1, Figure 5). Many of these fires burned during the entire ABLE 3A study period, and the aircraft intercepted a number of biomass burning plumes during the flights over Alaska.

Large smoke palls are often revealed by polar orbiter satellite imagery during the summer months over parts of Siberia (M. Matson, personal communication, 1991). Warm and dry conditions under the ridge of high pressure over eastern Asia (shown in Figure 2) likely contributed to an active fire season in that region as well. Airborne lidar and trajectory analyses for mission 14 on July 26 show evidence of a case of long-range transport of smoke from Asia to Alaska.

MISSION DISCUSSIONS

Missions 1 and 2: July 7, 1988, Wallops Flight Facility, Virginia, to Churchill, Manitoba, via Thunder Bay, Ontario. For mission 1, the dominating synoptic feature was a strong ridge of high pressure which had been stagnant over the Great Lakes region for several days prior to the flight. The major feature affecting mission 2 was a strong area of low pressure centered over northern Saskatchewan, with an associated surface frontal system over Manitoba and Ontario.

Trajectories for mission 1 depict the anticyclonic flow of continental air over the Great Lakes region (Figure 6). For the first half of mission 2, anticyclonic flow around the edge of the Great Lakes high was evident, with continental air coming from the central United States. During the second half of the mission, transport was associated with the Saskatchewan low, with a flow of modified mP air moving from the northwest coast of the United States toward northern Manitoba.

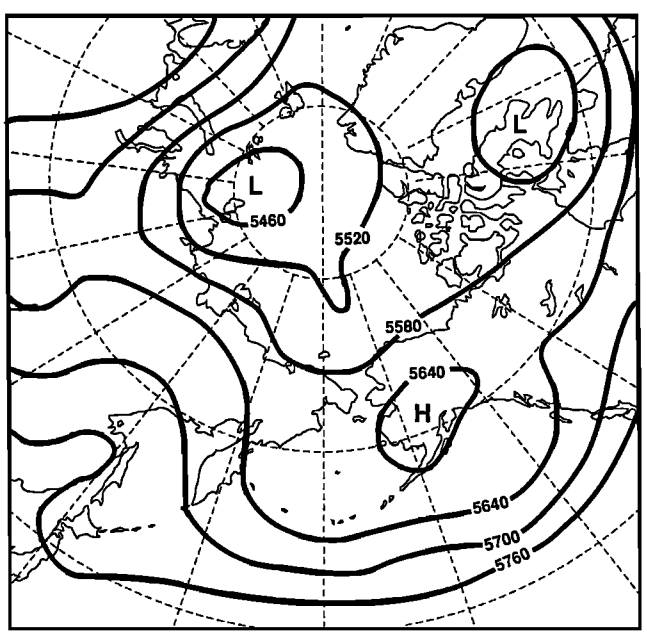

Fig. 2. As in Figure 1, but for July 1988 only.

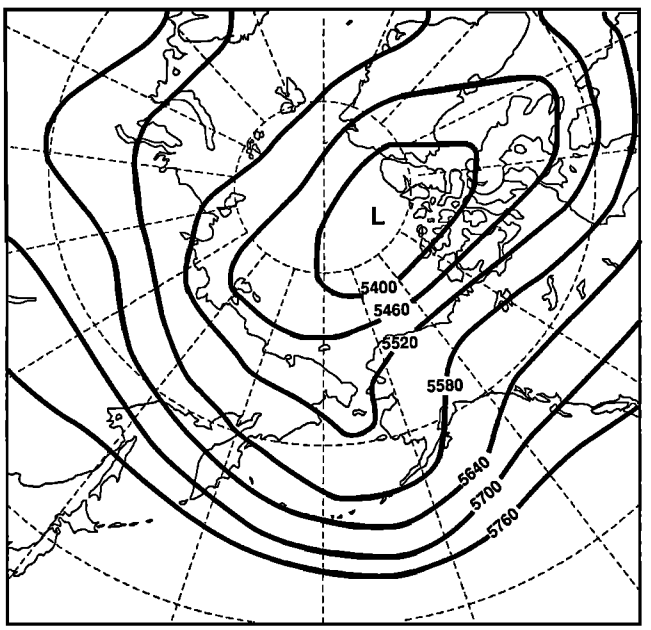

Fig. 3. As in Figure 1, but for August 1988 only.

On mission 1, the sampled mid-tropospheric air was relatively dry, a result of the strong subsidence occurring with the Great Lakes ridge. A cross section (not shown) constructed from rawinsonde reports along the flight path showed this dry air, which existed above a well-defined moisture gradient at 700 hPa (the top of the deep surface haze layer).

During mission 2, as the aircraft flew in the vicinity of the frontal zone over western Ontario, very moist air was encountered. Very low dew points (−30° to −50°C) were then observed as the aircraft was over Manitoba. A cross section (not shown) along the flight path revealed a wind velocity maximum (the polar jet stream) and a perturbed tropopause between Big Trout Lake, Ontario (53°50′N, 89°52′W) and Churchill, Manitoba (58°45′N, 94°04′W). This, along with high values of potential vorticity over that region, suggests the presence of stratospheric air in the middle troposphere.

Mission 3: July 8, 1988, Churchill, Manitoba, to Thule, Greenland. A strong polar vortex was positioned over the North Pole, with a southward extension of this vortex located over the Baffin Island/southern Greenland region. A ridge of high pressure was situated between these two lows. In addition, the low which had affected conditions during mission 2 was weakening and becoming stationary over northern Manitoba.

Trajectories (Figure 7) show an initial eastward transport of cP air across the Arctic Ocean around the strong polar vortex. This air then turned toward the south as circulation around the Baffin Island low intensified.

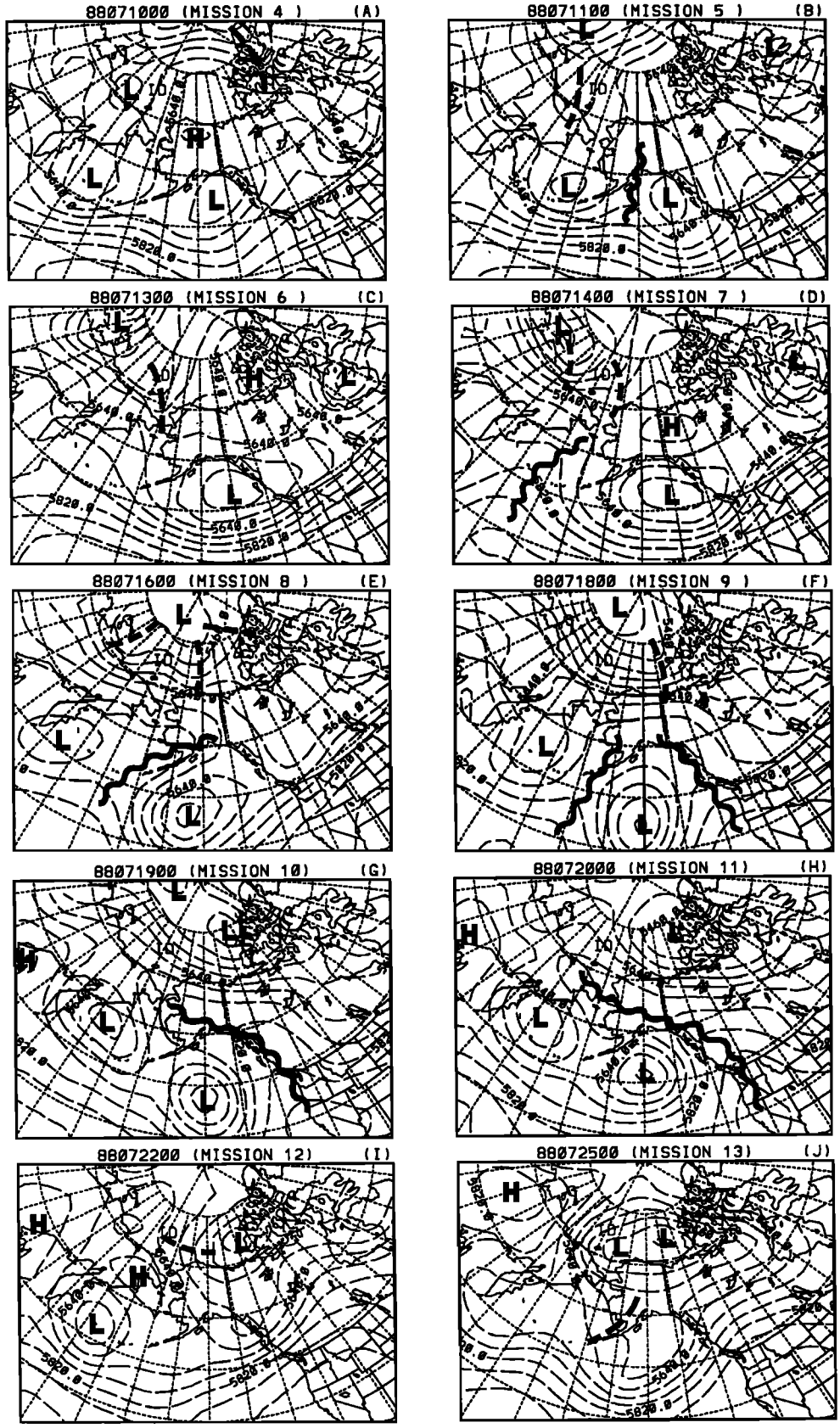

Fig. 4. Daily maps of the 500 hPa height field for each of the days when flight missions were conducted over Alaska. Centers of low (L) and high (H) pressure are shown, as well as the axes of troughs of low pressure (heavy dashed lines) and ridges of high pressure (heavy jagged lines).

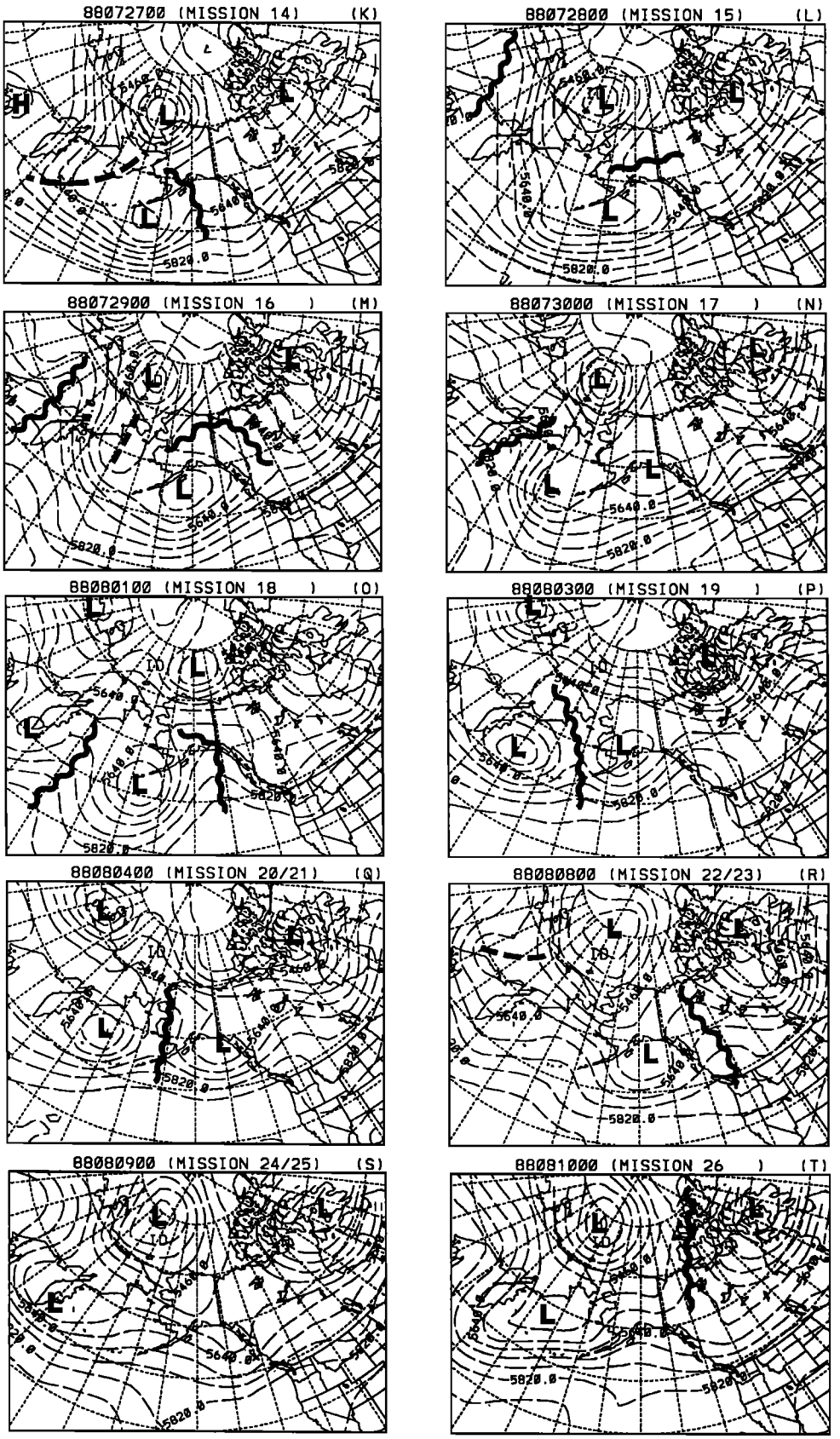

Fig. 4. (continued)

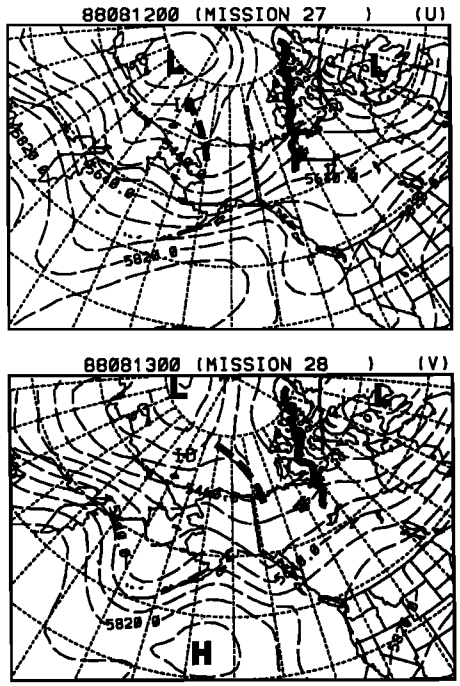

Fig. 4. (continued)

One area of low dew points (below −25°C) was sampled over the northern end of Hudson Bay, while a second, more extensive area of very low dew points (−40° to −50°C) was observed over Baffin Island. Narrow fingers of enhanced ozone extending from the tropopause down to altitudes below 7 km were detected by aircraft lidar (not shown), and high values of potential vorticity were analyzed over that region, confirming that air of stratospheric origin was encountered.

Mission 4: July 9, 1988, Thule, Greenland, to Fairbanks,

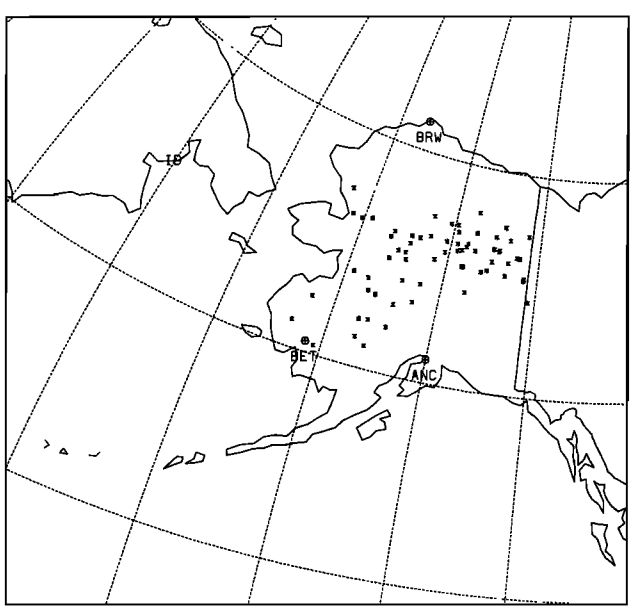

Fig. 5. Locations of major fires (burn areas >4000 m^2 or 100 acres) reported by the Alaska Fire Service during ABLE 3A. Barrow (BRW), Bethel (BET), and Anchorage (ANC) station locations are also shown.

TABLE 1. Location, Duration, and Size of Major 1988 Alaskan Fires (Over 100 Acres)

Latitude	Longitude	Date in 1988 Start	Date in 1988 End	Acres Burned
64.42	147.39	April 16	Sept. 2	13,780
65.12	156.00	May 29	June 11	2,550
66.00	154.27	June 10	June 14	200
66.54	159.02	June 15	Sept. 9	207,800
67.46	162.12	July 6	Aug. 2	14,167
66.04	156.49	July 6	Aug. 30	8,080
63.47	157.11	July 12	Sept. 2	83,300
65.55	154.50	July 12	Aug. 1	3,150
66.40	160.09	July 12	Aug. 2	3,680
63.39	156.30	July 12	Oct. 12	25,250
64.01	157.46	July 13	Sept. 2	52,600
66.32	156.24	July 13	Aug. 31	11,714
64.11	159.06	July 14	July 21	900
65.56	155.30	July 15	Aug. 31	16,700
62.47	162.14	July 19	July 30	650
66.46	161.16	Aug. 8	Aug. 13	350
60.27	150.58	May 26	June 1	355
60.37	160.55	May 22	May 26	700
61.18	163.21	June 30	July 2	100
61.00	156.01	July 3	Aug. 13	32,985
62.08	154.43	July 11	Aug. 9	5,320
62.21	156.32	July 12	Aug. 24	89,850
62.13	157.16	July 14	Aug. 13	330
63.16	154.30	July 15	Aug. 9	650
61.32	157.08	July 19	July 27	130
66.00	145.07	June 27	Aug. 4	2,880
66.34	142.38	June 28	Oct. 10	8,520
65.47	146.08	June 28	Aug. 4	26,000
65.58	145.49	June 29	Oct. 1	289,360
67.13	147.24	June 29	Aug. 22	2,950
67.35	141.30	June 30	July 23	300
66.50	144.49	June 30	July 2	2,560
66.56	145.07	June 30	Oct. 1	4,070
66.56	145.02	July 4	Oct. 1	9,300
67.59	144.10	July 14	Oct. 1	16,500
66.58	148.04	July 14	Oct. 1	35,500
66.43	148.13	July 14	Oct. 1	58,200
67.12	145.00	July 16	Oct. 1	36,700
66.34	147.12	Aug. 1	Oct. 1	14,510
65.47	143.43	Aug. 9	Aug. 21	160
64.35	152.12	July 14	June 15	100
67.01	149.32	June 15	Aug. 11	8,000
66.35	153.35	June 15	June 18	170
67.30	149.51	June 15	July 11	230
66.49	150.40	June 25	July 11	140
63.47	152.51	July 5	July 9	150
65.26	154.27	July 12	Sept. 30	141,546
66.54	152.27	July 12	July 29	275
67.42	152.40	July 13	Aug. 11	1,500
66.34	154.29	July 14	July 29	910
67.29	150.34	July 15	Aug. 8	280
64.33	154.02	July 16	Aug. 22	850
65.59	151.27	July 27	Aug. 21	620
66.00	150.35	Aug. 1	Sept. 30	12,060
65.54	148.07	June 11	Oct. 1	541,231
64.40	140.59	June 11	June 24	400
66.50	149.17	June 12	June 24	1,245
65.35	141.38	June 13	June 28	400
65.54	148.21	June 14	June 19	300
66.05	143.27	June 14	Oct. 1	180
65.43	141.32	June 15	June 28	340
66.31	142.02	June 15	June 20	130
66.56	144.42	June 15	Oct. 1	105,000
66.19	149.01	June 26	Oct. 1	24,380
66.26	148.58	June 26	Oct. 1	64,800
67.06	143.36	June 27	Oct. 1	144,000
68.02	147.40	June 27	July 14	220

Total number of fires is 67; total acres burned is 2,132,258.

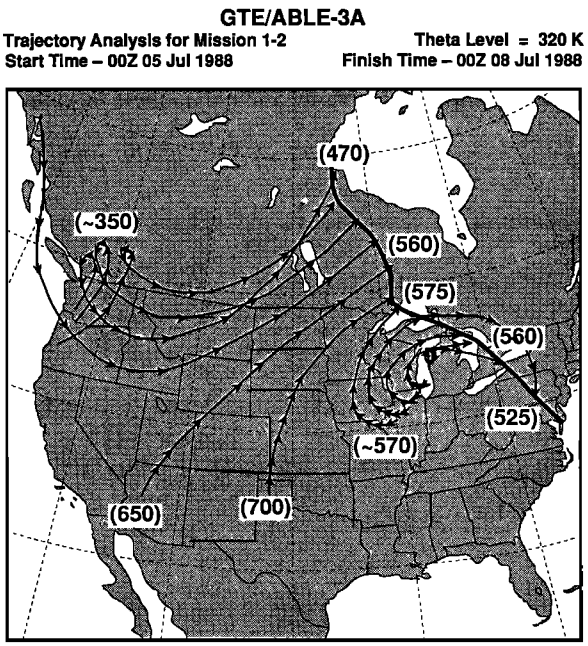

Fig. 6. The 320 K trajectory paths for air arriving along the flight path during missions 1 and 2. Trajectory start time is 0000 UTC on July 5, 1988; trajectory end time is 0000 UTC on July 8, 1988. Arrows along each trajectory path show 6-hour positions of the air parcels. Heavy solid line denotes the aircraft flight path. Representative values of beginning and ending trajectory pressures (in hectopascals) are also depicted.

Alaska. The intense polar vortex remained over the Arctic Ocean between Greenland and the North Pole. A short-wave trough of low pressure was rotating around this vortex, moving across the Queen Elizabeth Islands (Figure 4*a*). In addition, a weak ridge of high pressure resided over interior Alaska.

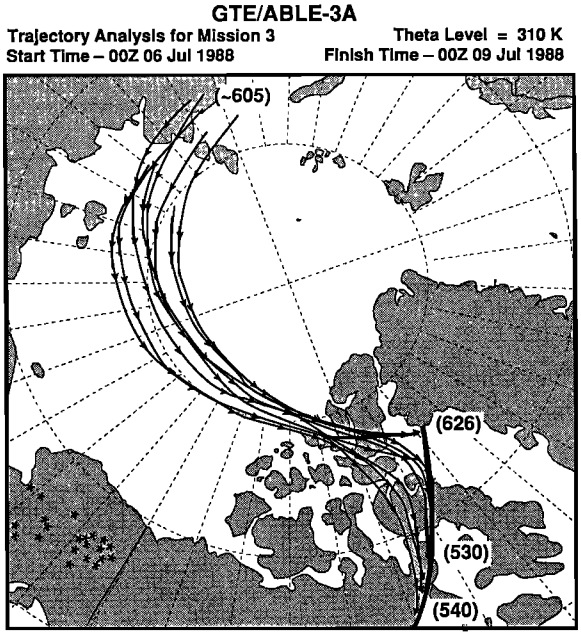

Fig. 7. The 310 K trajectory paths for air arriving along the flight path during mission 3. Trajectory start time is 0000 UTC on July 6, 1988; trajectory end time is 0000 UTC on July 9, 1988.

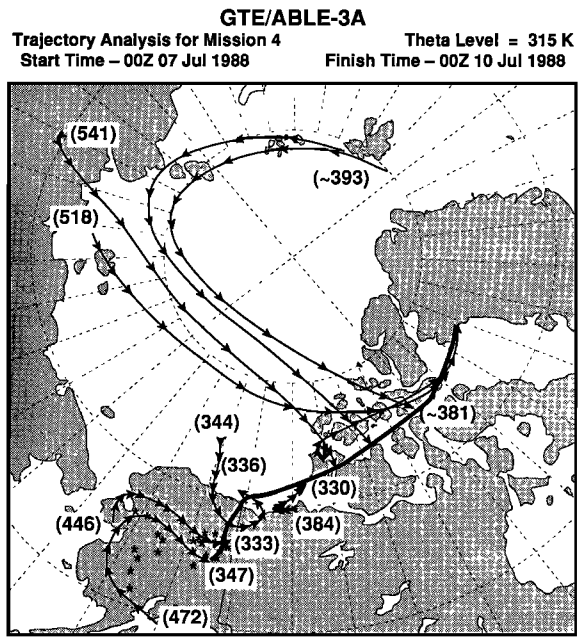

Fig. 8. The 315 K trajectory paths for air arriving along the flight path during mission 4. Trajectory start time is 0000 UTC on July 7, 1988; trajectory end time is 0000 UTC on July 10, 1988. Asterisks denote locations of major Alaskan fires (>4000 m^2) burning during the trajectory time period.

Trajectories (Figure 8) indicate that cP air sampled during the first half of the flight leg (Thule to Banks Island) had been transported across the Arctic Ocean by the circulation of the polar vortex. From Banks Island to Fairbanks, the weaker transport associated with the ridge over Alaska is evident by the much shorter trajectory paths of cP air, which generally had resided over Alaska prior to the flight. Numerous fires had been burning in the Yukon Valley north of Fairbanks, and haze which was observed from the aircraft starting near 140°W longitude contained smoke from these fires [*Gregory et al.*, this issue; *Talbot et al.*, this issue], as well as pollution from the Prudhoe Bay oil field operations [*Blake et al.*, this issue].

Values of potential vorticity above the "stratospheric threshold" value of 10.0×10^{-5} K m^2 kg^{-1} s^{-1} [*Shapiro et al.*, 1987] were analyzed at 500 hPa in the region of the polar jet just north of the flight track (Figure 9). Airborne lidar measurements (Plate 1) show a well-defined tropopause fold along the southern edge of the jet, with deformation of the ozone and aerosol structure into the upper and middle troposphere (see *Browell et al.* [this issue] for details of lidar measurements during ABLE 3A).

Mission 5: July 10, 1988, Fairbanks, Alaska, to Barrow, Alaska. A weakening ridge of high pressure remained over interior Alaska, positioned between lows located over the Bering Sea and the Gulf of Alaska (Figure 4*b*).

Trajectories (Figure 10) indicate that the air sampled during this flight had resided over Alaska due to a very weak and erratic flow associated with the ridge of high pressure. During the 24 hours prior to the flight, a more organized southerly flow had become established over the Brooks Range as the ridge weakened and the Bering Sea low strengthened and moved eastward.

Active fires continued to burn in the Yukon Valley.

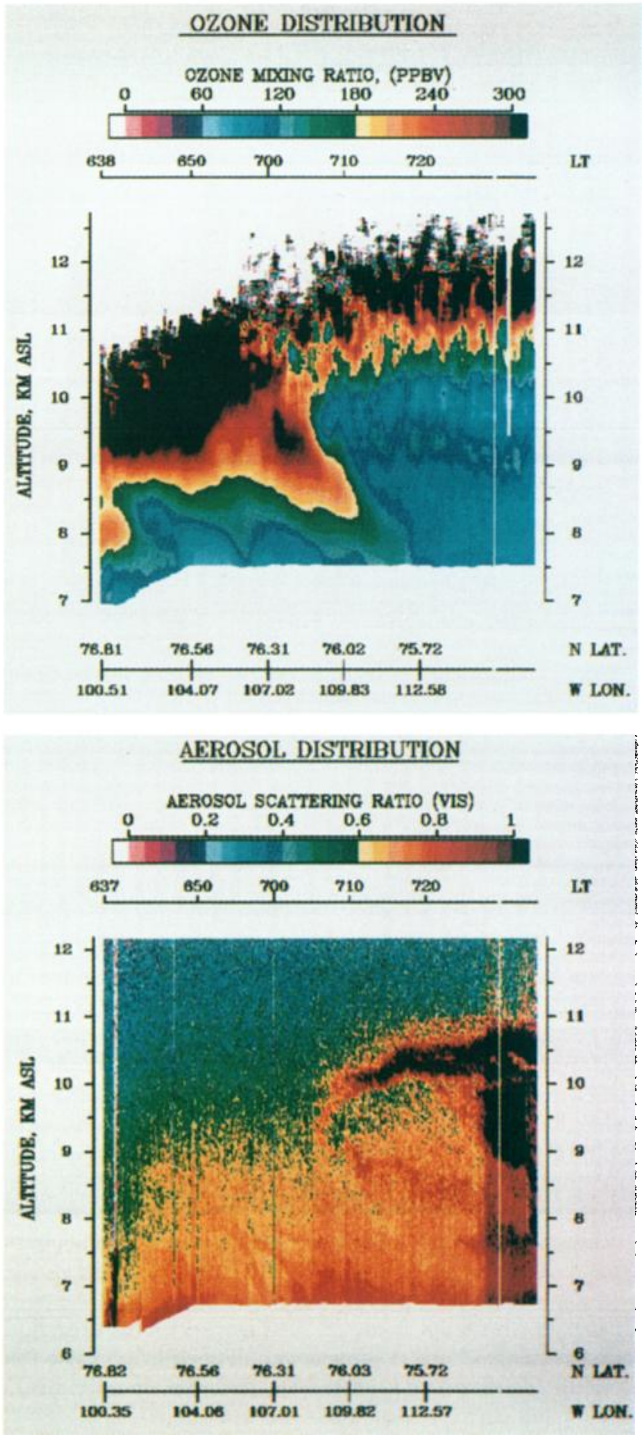

Plate 1. Airborne lidar measurements of ozone mixing ratio (top) and visible aerosol scattering ratio (bottom) in the vicinity of the polar jet during mission 4 on July 9, 1988. Local times (LT) displayed along the top of each panel are Alaskan Daylight Time (UTC − 8 hours).

Surface stations reported convective clouds over the Brooks Range during the flight, which could have led to vertical transport of fire smoke into the free troposphere.

Mission 6: July 12–13, 1988, photochemical flight, northeast of Barrow, Alaska. A shallow, cold cP air mass existed north of Alaska in conjunction with a ridge of high pressure which had been building over the Canadian Arctic

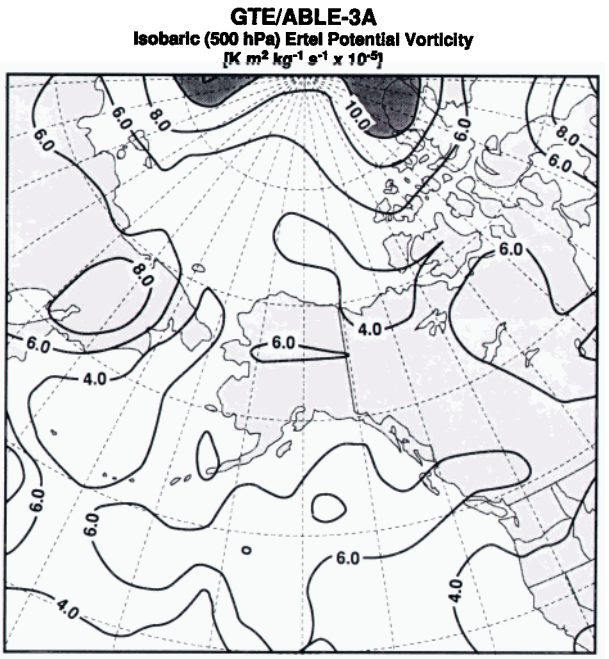

Fig. 9. Contours of Ertel potential vorticity ($\times 10^{-5}$ K m^2 kg^{-1} s^{-1}) along the 500 hPa surface for 1200 UTC on July 9, 1988. Values greater than 10.0 over the extreme northern portion of the Queen Elizabeth Islands (just north of the flight path) are indicative of stratospheric air.

Islands (Figure 4*c*). This cP air mass was slowly being displaced by a south-southwesterly flow of warmer cP air associated with a broad area of low pressure centered off the northern coast of Siberia.

In the lower troposphere, trajectories indicate the slow transport of cold cP air, originating over northwestern Canada or the interior of Alaska (Figure 11). At higher levels, trajectories begin to show the infiltration of warmer cP air which had been moving northward across western Alaska (Figure 12).

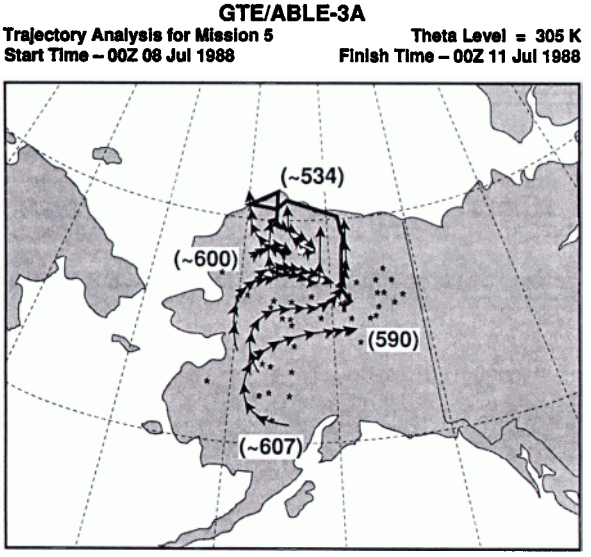

Fig. 10. The 305 K trajectory paths for air arriving along the flight path during mission 5. Trajectory start time is 0000 UTC on July 8, 1988; trajectory end time is 0000 UTC on July 11, 1988.

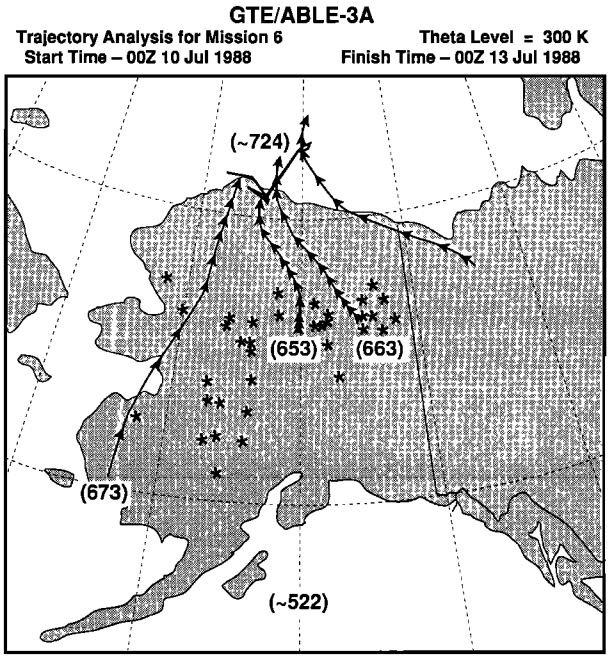

Fig. 11. The 300 K trajectory paths for air arriving along the flight path during mission 6. Trajectory start time is 0000 UTC on July 10, 1988; trajectory end time is 0000 UTC on July 13, 1988.

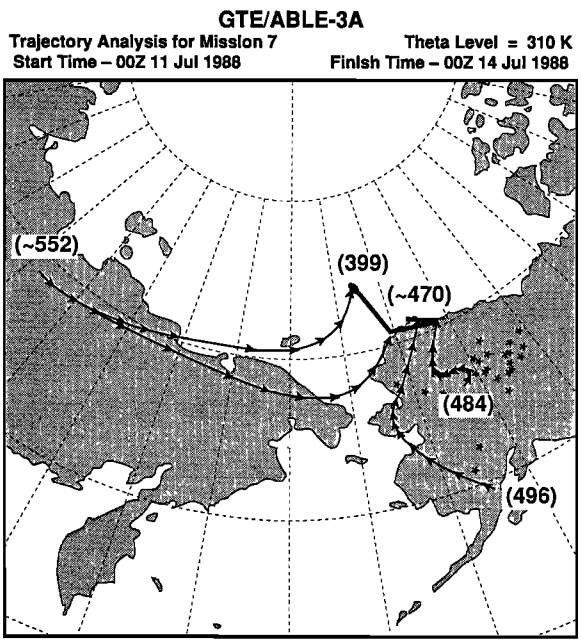

Fig. 13. The 310 K trajectory paths for air arriving along the flight path during mission 7. Trajectory start time is 0000 UTC on July 11, 1988; trajectory end time is 0000 UTC on July 14, 1988.

Mission 7: July 13–14, 1988, "whale-tundra watch," west of Barrow, Alaska. A polar vortex had begun to intensify along the Siberian coast (Figure 4*d*). A weak short-wave trough of low pressure was rotating around the vortex and moving toward the Barrow area. In addition, a ridge of high pressure had been building across Alaska from northwestern Canada.

Trajectories for all flight levels show that cP air in the immediate vicinity of Barrow had moved northward over Alaska (Figure 13). Air arriving over the Arctic Ocean had originated over Siberia and was transported eastward with the short wave.

Strong descending motion on the western edge of the Barrow short wave was responsible for stratosphere/troposphere exchange in that region. Airborne lidar (not shown) revealed enhanced ozone structure in the upper troposphere along the northernmost portions of the flight leg over the Arctic Ocean. The presence of air of stratospheric origin was also supported by high potential vorticity values

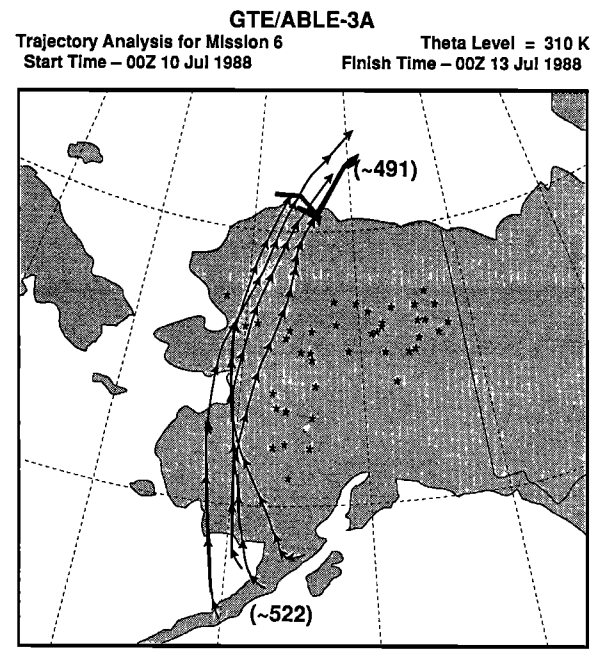

Fig. 12. The 310 K trajectory paths for air arriving along the flight path during mission 6. Trajectory start time is 0000 UTC on July 10, 1988; trajectory end time is 0000 UTC on July 13, 1988.

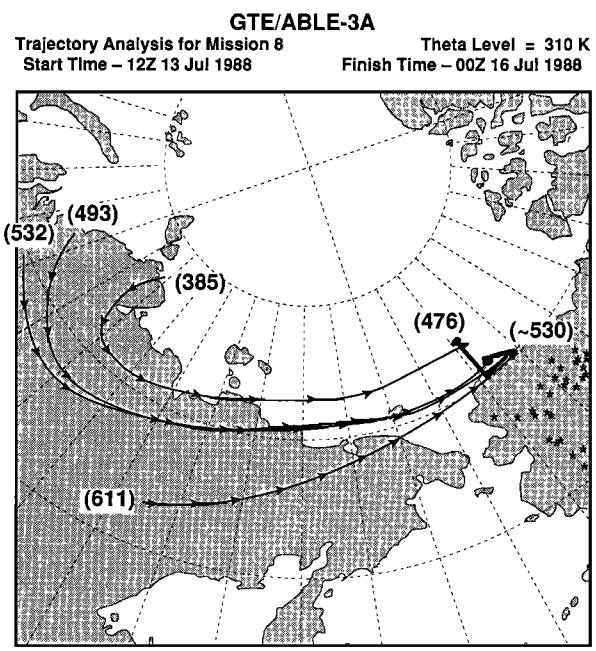

Fig. 14. The 310 K trajectory paths for air arriving along the flight path during mission 8. Trajectory start time is 0000 UTC on July 13, 1988; trajectory end time is 0000 UTC on July 16, 1988.

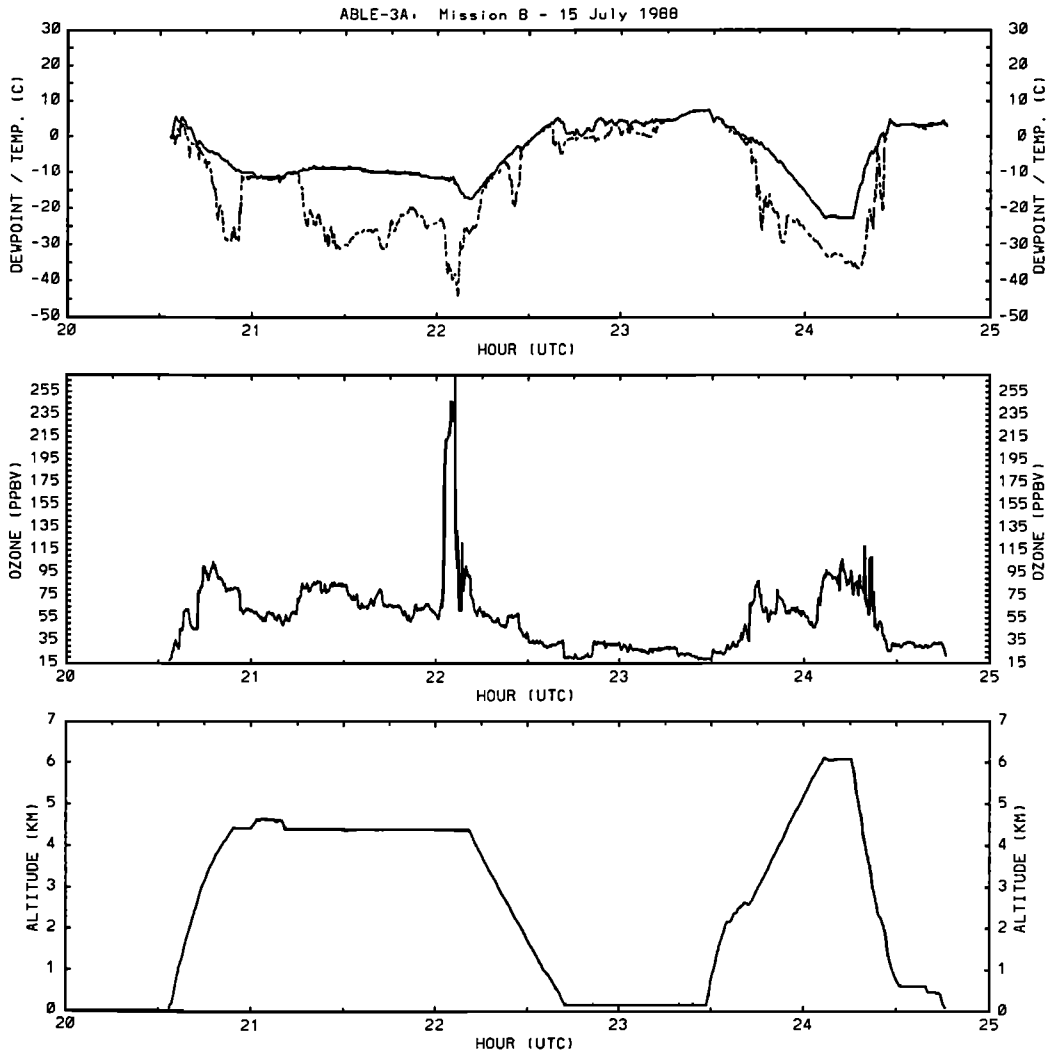

Fig. 15. In situ aircraft measurements of (top) temperature (solid line, degrees Celsius) and dew point (dashed line, degrees Celsius), (middle) ozone concentration (ppbv), and (bottom) pressure altitude (kilometers) during mission 8 on July 15, 1988. Time (hours UTC) is displayed along the abscissa of each plot. Note the dramatic increase in ozone concentration shortly after 2200 UTC, with a corresponding drop in the dew point.

(just above the "stratospheric threshold") analyzed at levels near the maximum altitude of the aircraft.

Mission 8: July 15–16, 1988, "whale-tundra watch," east of Barrow, Alaska. The polar vortex remained along the Siberian coast as the second in a series of short-wave troughs moved west to east across the Arctic Ocean north of Barrow (Figure 4*e*). Trajectories at all levels depict the strong westerly flow of cP air which originated over northern Siberia (Figure 14). This second short wave was more intense than the one affecting the previous mission, as evidenced by the longer trajectory transport paths (stronger winds).

The aircraft flew into the "dry slot" immediately behind the short wave. In situ aircraft measurements (Figure 15) revealed pronounced drying aloft as the wave axis was crossed around 2115 UTC during the westbound leg of the flight. Near the end of the northbound leg of the flight (2140–2210 UTC), the aircraft sampled colder and significantly dryer air with temperatures below −15°C and dew points less than −40°C. In addition, the highest in situ ozone levels observed during ABLE 3A were encountered [*Gregory et al.*, this issue], with concentrations in excess of 250 ppbv.

Lidar measurements (not shown) showed the middle and upper troposphere to be ozone rich, with mixing ratios in excess of 80 ppbv as low as 6 km. "Stratospheric threshold" values of potential vorticity north of Barrow suggest that stratospheric air existed down to levels near the highest aircraft altitude (4.5–6.0 km). *Sandholm et al.* [this issue] point out that the 3-day back trajectories originated near 385 hPa in the vicinity of the intensifying polar vortex, a region of very high potential vorticity (5 times greater than the "stratospheric threshold") 72 hours prior to the mission. This high potential vorticity did not appear to be conserved during the 3-day transport eastward toward Alaska, but levels of ozone and reactive nitrogen oxides (NO_y) were near those expected of stratospheric air.

Mission 9: July 17, 1988, "stair steps," northeast of Barrow, Alaska. The intense polar vortex persisted over the Arctic Ocean north of Siberia, with the third in a series of short-wave troughs located north and east of Barrow (Figure 4*f*). Trajectories at all levels again depict the strong

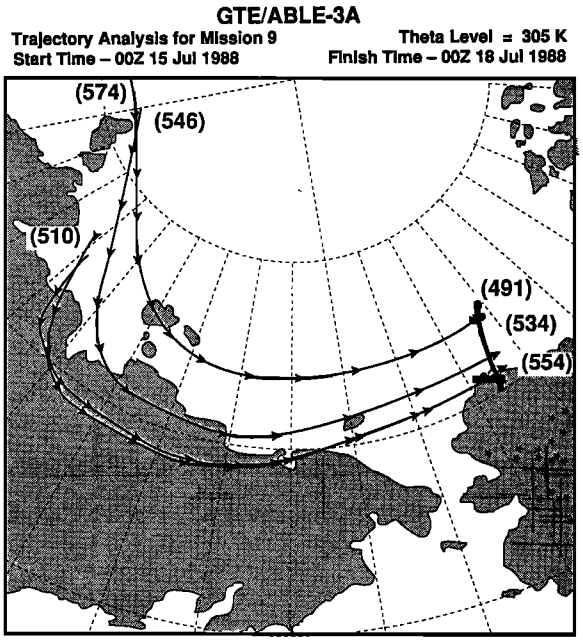

Fig. 16. The 305 K trajectory paths for air arriving along the flight path during mission 9. Trajectory start time is 0000 UTC on July 15, 1988; trajectory end time is 0000 UTC on July 18, 1988.

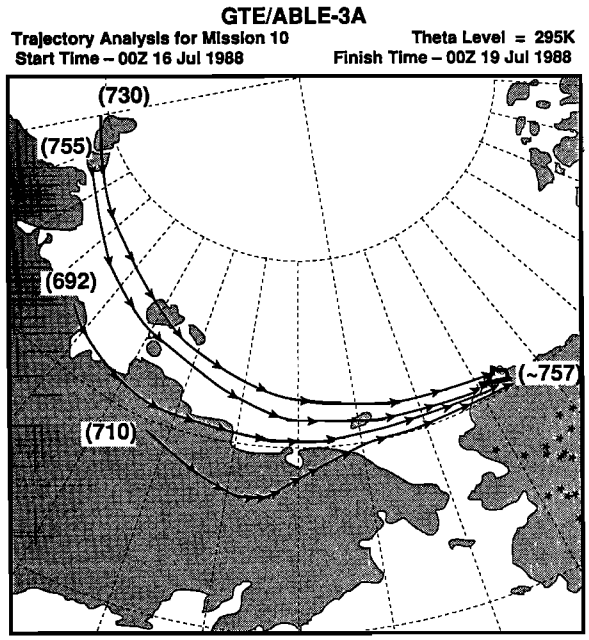

Fig. 17. The 295 K trajectory paths for air arriving along the flight path during mission 10. Trajectory start time is 0000 UTC on July 16, 1988; trajectory end time is 0000 UTC on July 19, 1988.

westerly flow of cP air which originated over northern Siberia, similar to that observed during mission 8 (Figure 16).

The aircraft flew toward the "dry slot" behind the exiting short wave. A cross section (not shown) depicted the polar jet stream and associated tropopause fold in the vicinity of the wave axis, and potential vorticity analyses suggested that stratospheric air existed in the upper troposphere over the Arctic Ocean. Airborne lidar (not shown) showed that the tropopause dropped from 9.5 km to 8.5 km during the flight leg over water, and well-defined structures in the ozone mixing ratio were seen extending down to levels below 8 km.

Mission 10: July 18–19, 1988, flux flight, south of Barrow, Alaska. The strong polar vortex over the Arctic Ocean had begun to split into two lobes, one just west of the Canadian Arctic Islands, and the other off the Siberian coast (Figure 4*g*). A ridge of high pressure had been building over southern Alaska during the previous 3–5 days. Trajectories for this flight indicate that the aircraft sampled a westerly flow of cP air, which again originated over northern Siberia and adjacent areas of the Arctic Ocean (Figure 17).

Mission 11: July 19–20, 1988, ocean/land spirals, south and west of Barrow, Alaska. A lobe of the polar vortex had become stationary over the Canadian Arctic Islands (Figure 4*h*). The ridge which had been building over southern Alaska was beginning to move northwestward into extreme eastern Siberia. Trajectories at all levels once again depict the westerly flow of cP air which originated over northern Siberia and adjacent areas of the Arctic Ocean (Figure 18). This flow regime was similar to that of the previous three missions, a result of the intensification and eastward migration of the extensive polar vortex across the Arctic Ocean which began July 13.

Bakwin et al. [this issue] noted a thick haze over the Bethel site during the day, likely due to smoke-laden air trapped by subsidence within the southern Alaska ridge. Trajectories arriving at Bethel near the surface (not shown) indicated that mP air had moved northward from the Alaska Peninsula, then stagnated in the vicinity of Bethel 12–24 hours prior to the flight. Trajectories at higher levels (also not shown) had been moving westward from the Anchorage area across the Alaska Range, passing over active fires.

Mission 12: July 21–22, 1988, ocean/land spirals, north and southwest of Barrow, Alaska. The polar vortex remained stationary over the Canadian Arctic Islands, and was responsible for a northerly flow of cP air across the Barrow

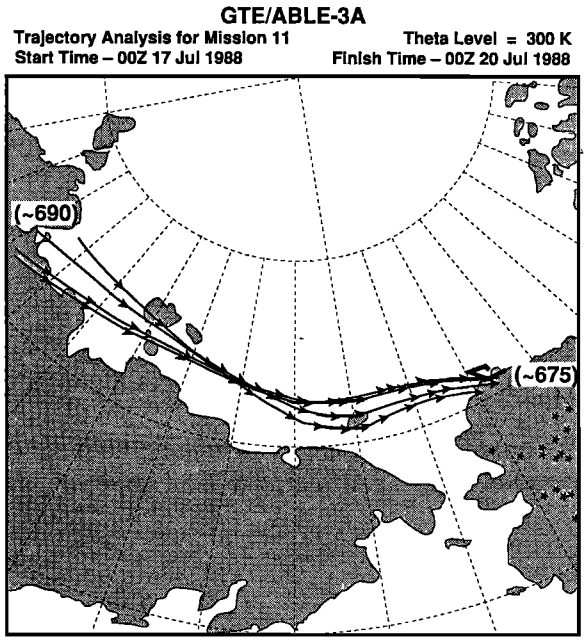

Fig. 18. The 300 K trajectory paths for air arriving along the flight path during mission 11. Trajectory start time is 0000 UTC on July 17, 1988; trajectory end time is 0000 UTC on July 20, 1988.

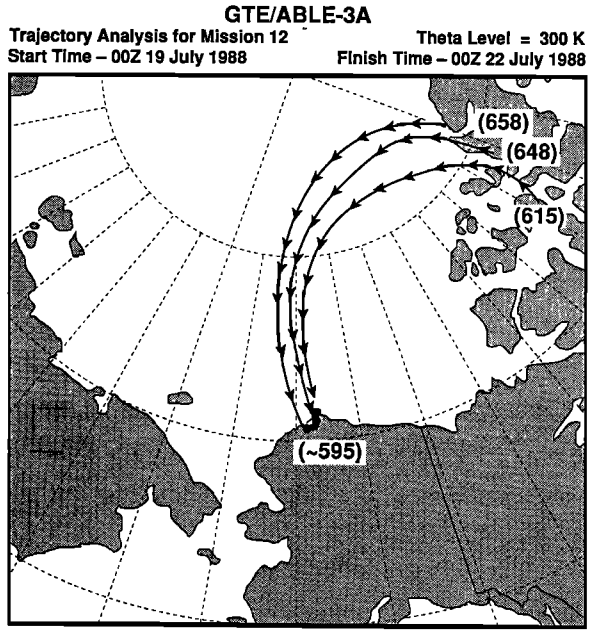

Fig. 19. The 300 K trajectory paths for air arriving along the flight path during mission 12. Trajectory start time is 0000 UTC on July 19, 1988; trajectory end time is 0000 UTC on July 22, 1988.

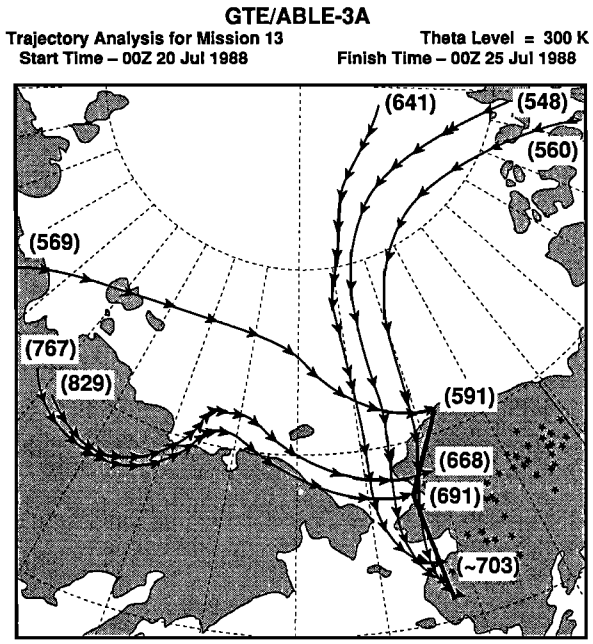

Fig. 21. The 300 K trajectory paths (5-day) for air arriving along the flight path during mission 13. Trajectory start time is 0000 UTC on July 20, 1988; trajectory end time is 0000 UTC on July 25, 1988.

region (Figure 4*i*). Low-level trajectories indicate the counterclockwise transport around the low, originating in the vicinity of the Queen Elizabeth Islands (Figure 19). Higher in the troposphere, some of the air is shown to have originated near the northern coast of Siberia (Figure 20). This type of transport over the Arctic Ocean icepack towards Barrow was unique to this particular mission.

Mission 13: July 24, 1988, Barrow, Alaska, to Bethel, Alaska. The polar vortex was becoming elongated off the northwest coast of Alaska (Figure 4*j*). In addition, a shortwave trough in the upper troposphere was moving southeastward across the Yukon/Kuskokwim delta region.

In the lower to middle troposphere, the cP air mass along the northern portion of the flight is shown to have originated over Siberia (Figure 21). During the remainder of the flight, the depicted source region was over the ice pack, north of Alaska and Siberia. At levels near the maximum aircraft altitude, trajectories along the entire flight path indicate transport from central and eastern Siberia (Figure 22). Potential vorticity analyses suggest that air of stratospheric origin was evident in the middle and upper troposphere near Barrow.

During the afternoon hours, smoke from fires was reducing the surface visibility at Bethel and Galena. Airborne lidar (not shown) detected the presence of layers at altitudes near 2–3 km exhibiting high ozone correlated with high aerosol concentrations, characteristic of biomass burning plumes.

Mission 14: July 26–27, 1988, spirals near Bethel, Alaska. A broad long-wave trough of low pressure had formed across the Bering Sea as the polar vortex intensified off the northwest coast of Alaska (Figure 4*k*). A weak ridge of high pressure was building aloft over southern Alaska, keeping the middle troposphere relatively dry.

Low-level trajectories show that mP air had moved eastward across the Bering Sea towards the Bethel region (Figure 23). At higher levels, transport from northern Siberia was indicated (Figure 24).

Lidar detected the presence of thin layers of high aerosol scattering near 2000, 3000–3500, and 4000 m (Plate 2). It is likely that the lowest (and thickest) haze layer consisted of residual smoke from fires that had been burning in the area during the previous several days, while the higher (and much thinner) layers had been transported from Siberia and were trapped just below subsidence layer temperature inversions.

Mission 15: July 27–28, 1988, "wall flight," northeast of

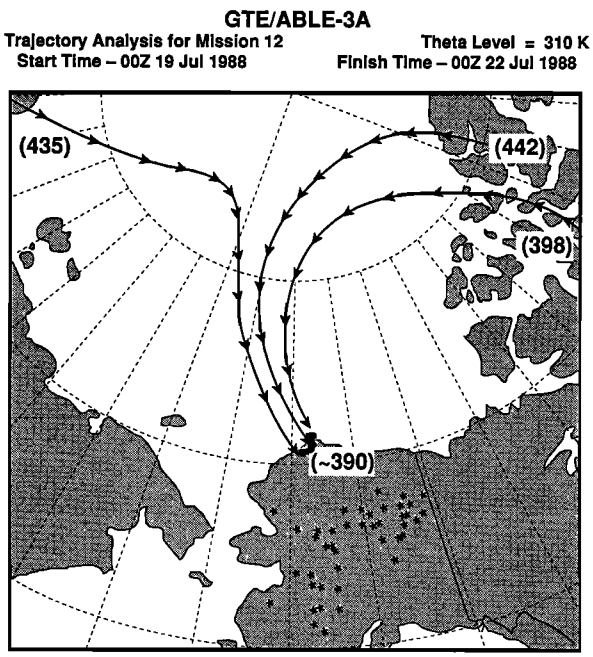

Fig. 20. The 310 K trajectory paths for air arriving along the flight path during mission 12. Trajectory start time is 0000 UTC on July 19, 1988; trajectory end time is 0000 UTC on July 22, 1988.

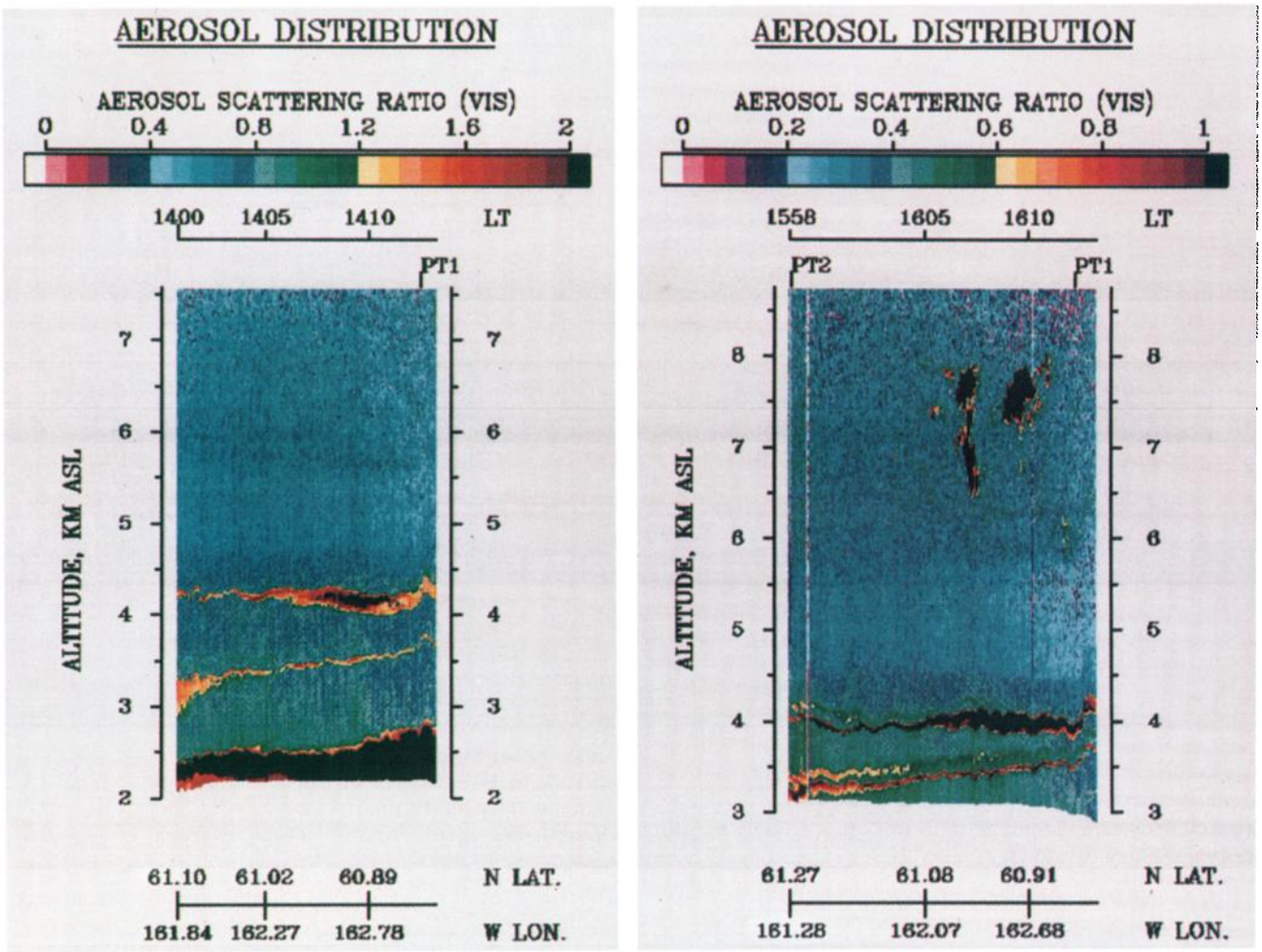

Plate 2. Airborne lidar measurements of visible aerosol scattering ratios during mission 14 on July 26–27, 1988. Local times (LT) displayed along the top of each panel are Alaskan Daylight Time (UTC − 8 hours). Note the thin vertical structure of the elevated haze/smoke plumes.

Bethel, Alaska. The counterclockwise flow associated with the Bering Sea trough of low pressure was transporting mP air into southwestern Alaska (Figure 4*l*). Low-level trajectories show that this air had been moving eastward across the Bering Sea, then northward over the flight region (Figure 25). High-level trajectories depict transport from the Arctic Ocean and extreme northern Siberia (Figure 26). The weak ridge of high pressure persisted over central Alaska, sustaining the dry air throughout the mid-troposphere.

The lower troposphere was convectively unstable across interior Alaska, and moderate cumulus buildups were reported to the distant northeast of Bethel, transporting fire smoke upward into the middle troposphere.

Mission 16: July 28–29, 1988, flux flight, near Bethel, Alaska. A weak low was drifting north-northeastward across the Gulf of Alaska, while the ridge that had been situated over central Alaska was beginning to migrate northward (Figure 4*m*). Trajectories show that mP air had moved northward from the Gulf of Alaska, then north-westward towards the Bethel region (Figure 27). Rawinsonde reports indicated that this mP air mass contained higher moisture throughout the middle troposphere, as compared to the previous two missions. This difference in moisture profile resulted from the residence time of this air mass over the warmer waters of the Gulf of Alaska versus the colder Bering Sea.

At the surface, a north-to-south oriented trough was moving westward across the Alaska Range. During the flight, two lines of cumulus with embedded rainshowers formed in response to this migrating trough, once again introducing the likelihood of vertical transport of smoke from active fires in the Alaska Range region.

Mission 17: July 29–30, 1988, land-sea interface, south of Bethel, Alaska. The Gulf of Alaska low was weakening as it moved inland across extreme southeastern Alaska (Figure 4*n*). Trajectories show that mP air had moved northward from the Gulf of Alaska, then westward over the flight region (Figure 28). Air arriving along the northern portion of the flight track was shown to have had a significant residence time over land. Bethel rawinsonde reports revealed that this mP air mass was moist at all levels of the mixed layer and free troposphere.

Mission 18: July 31, 1988, flux flight 2, near Bethel, Alaska. A strong Bering Sea low had been drifting eastward to the vicinity of the Alaska Peninsula (Figure 4*o*). Trajectories depict the slow transport of mP air northward

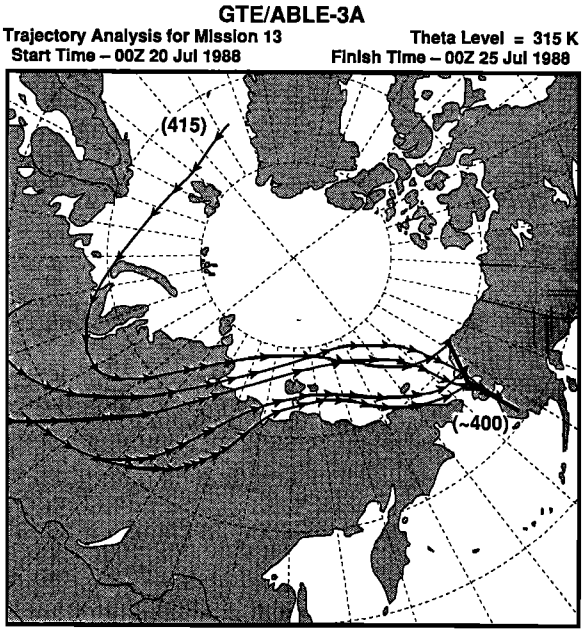

Fig. 22. The 315 K trajectory paths (5-day) for air arriving along the flight path during mission 13. Trajectory start time is 0000 UTC on July 20, 1988; trajectory end time is 0000 UTC on July 25, 1988.

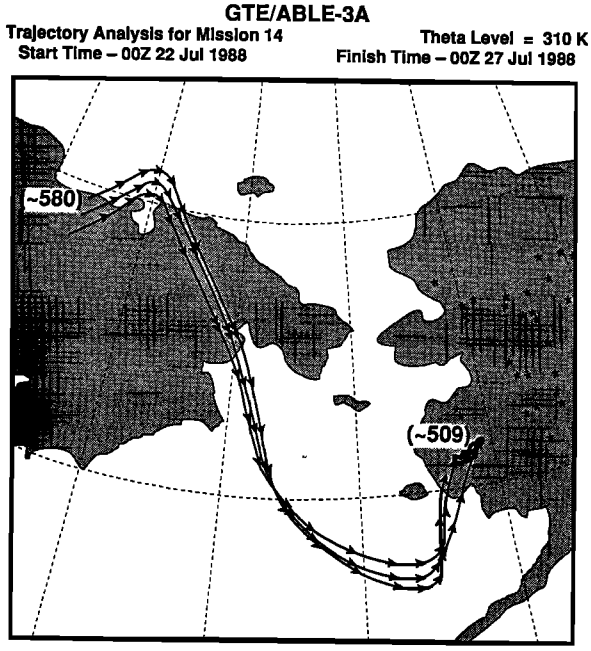

Fig. 24. The 310 K trajectory paths (5-day) for air arriving along the flight path during mission 14. Trajectory start time is 0000 UTC on July 22, 1988; trajectory end time is 0000 UTC on July 27, 1988.

toward Bethel (Figure 29). A ridge of high pressure had once again formed over the southern and central Alaskan interior, keeping the middle troposphere dry and stable across that region. However, an increase in mid-tropospheric moisture during the day was evident from Bethel rawinsondes, as the moist mP air was began to work its way north-northwestward.

Mission 19: August 2–3, 1988, land-sea interface, southwest of Bethel. The Bering Sea low was slowly moving inland over southwestern Alaska and weakening (Figure 4*p*). Low-level trajectories show that mP air had been moving northward from the northern Pacific and the Gulf of Alaska (Figure 30). Higher in the troposphere, trajectories depict a mixture of modified cP air moving from the coast of Siberia across the Bering Sea and mP air from the northern Pacific (Figure 31).

A strong but narrow ridge of high pressure existed across the eastern Bering Sea. Subsidence associated with this

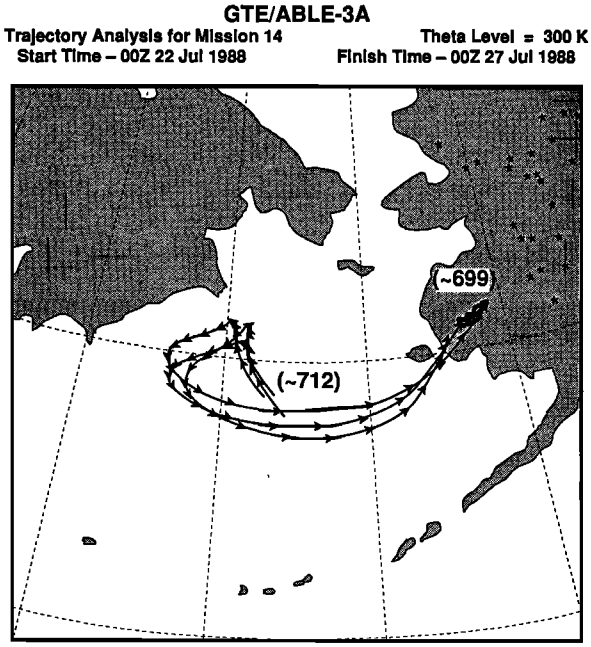

Fig. 23. The 300 K trajectory paths (5-day) for air arriving along the flight path during mission 14. Trajectory start time is 0000 UTC on July 22, 1988; trajectory end time is 0000 UTC on July 27, 1988.

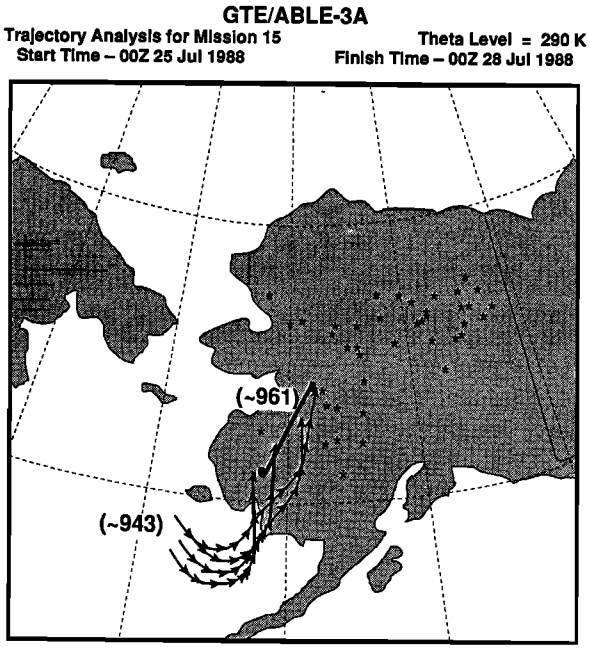

Fig. 25. The 290 K trajectory paths for air arriving along the flight path during mission 15. Trajectory start time is 0000 UTC on July 25, 1988; trajectory end time is 0000 UTC on July 28, 1988.

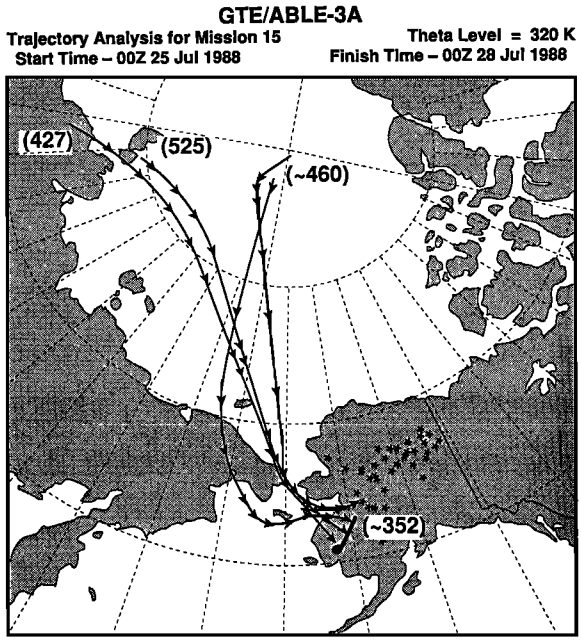

Fig. 26. The 320 K trajectory paths for air arriving along the flight path during mission 15. Trajectory start time is 0000 UTC on July 25, 1988; trajectory end time is 0000 UTC on July 28, 1988.

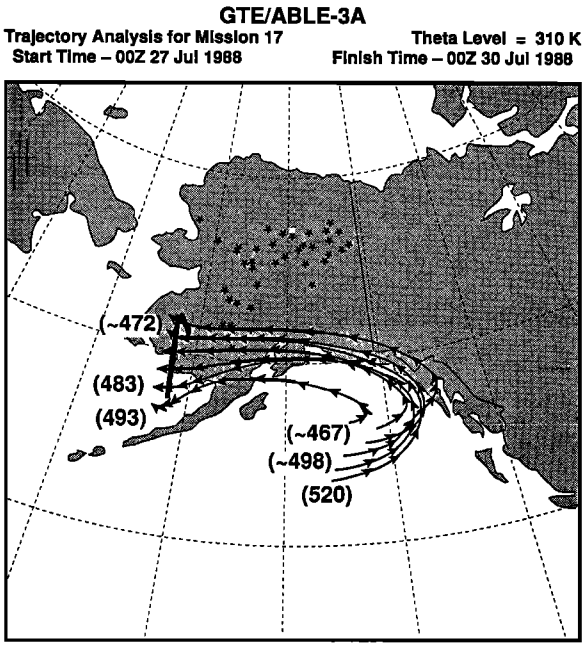

Fig. 28. The 310 K trajectory paths for air arriving along the flight path during mission 17. Trajectory start time is 0000 UTC on July 27, 1988; trajectory end time is 0000 UTC on July 30, 1988.

ridge was evident from the St. Paul Island rawinsonde, which showed a very dry and stable atmosphere between 1200 and 6000 m (4000–19,000 ft) over the Bering Sea. The effects of this strong subsidence were noted even at low levels, as large breaks in the extensive marine stratus deck appeared during the afternoon hours.

Numerous fires were reported burning to the distant east and northeast of Bethel, with one isolated fire to the distant northwest. Trajectories suggest that some smoke from these fires could have been advected toward the Bethel area during the day.

Missions 20 and 21: August 3–4, 1988, spirals near Bethel, Alaska. The ridge of high pressure over the Bering Sea had moved eastward into western Alaska (Figure 4*q*). Subsidence within this ridge was keeping the middle troposphere warm and dry, with light winds. The aging Bering Sea low was now located over extreme southeastern Alaska. Trajectories at high levels show that cP air which originated over

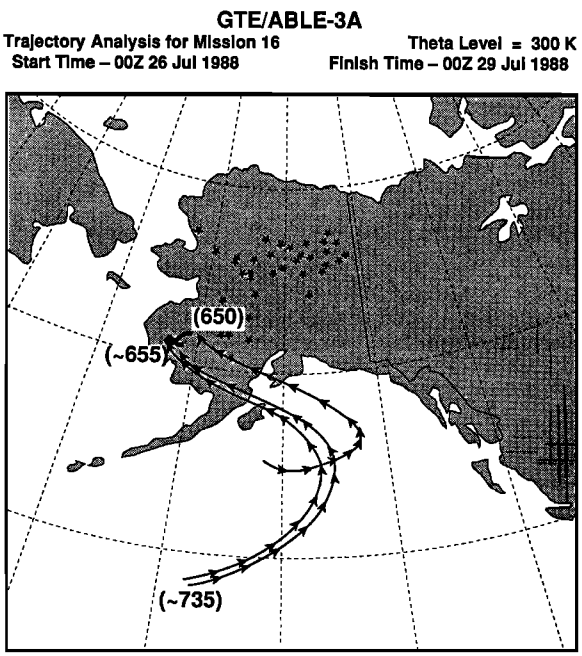

Fig. 27. The 300 K trajectory paths for air arriving along the flight path during mission 16. Trajectory start time is 0000 UTC on July 26, 1988; trajectory end time is 0000 UTC on July 29, 1988.

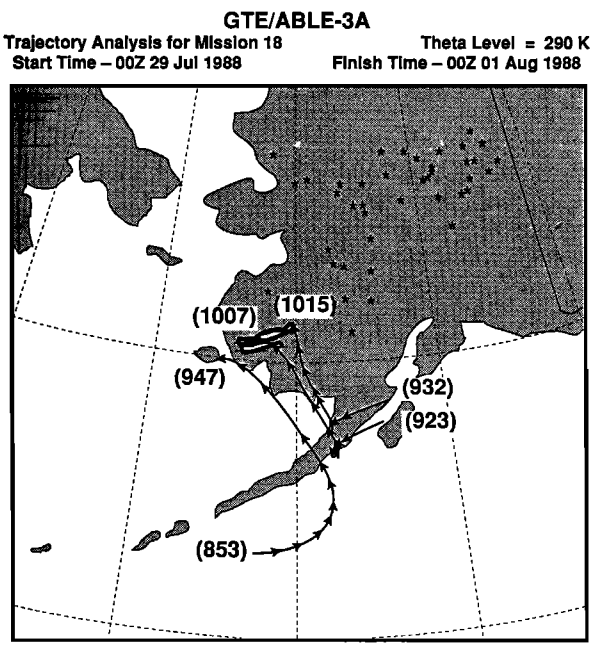

Fig. 29. The 290 K trajectory paths for air arriving along the flight path during mission 18. Trajectory start time is 0000 UTC on July 29, 1988; trajectory end time is 0000 UTC on August 1, 1988.

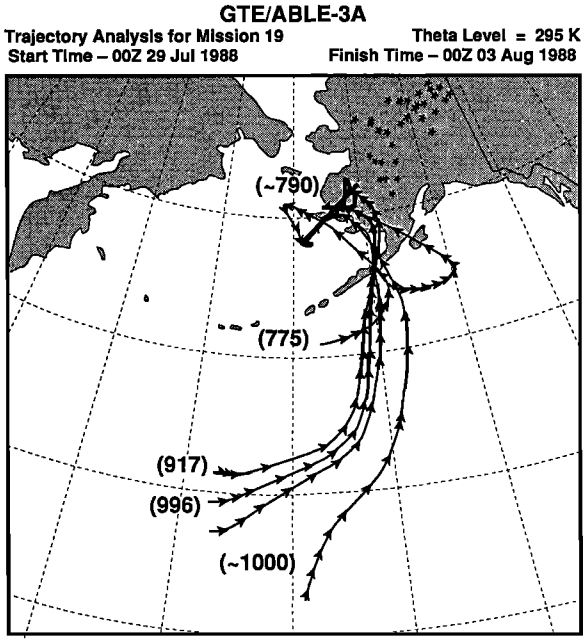

Fig. 30. The 295 K trajectory paths (5-day) for air arriving along the flight path during mission 19. Trajectory start time is 0000 UTC on July 29, 1988; trajectory end time is 0000 UTC on August 3, 1988.

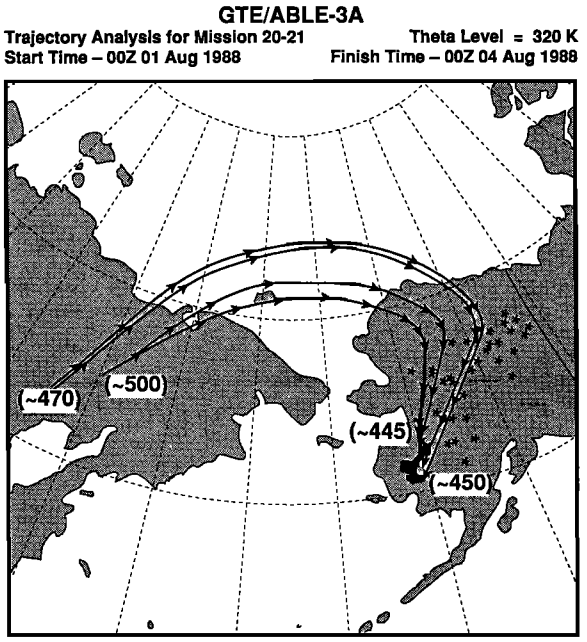

Fig. 32. The 320 K trajectory paths for air arriving along the flight path during missions 20 and 21. Trajectory start time is 0000 UTC on August 1, 1988; trajectory end time is 0000 UTC on August 4, 1988.

eastern Siberia had been transported eastward, then southward toward Bethel in association with the migrating ridge (Figure 32). At the lowest levels, a northward transport of mP air is indicated as the Bering Sea low moved eastward across the region (Figure 33). A combination of these two transport regimes was evident at intermediate altitudes (Figure 34).

During mission 20 (late morning to early afternoon, local time), aircraft temperature/dew point profiles revealed a stratified lower and middle troposphere. Multiple subsidence layer temperature inversions were noted at altitudes between 2500 and 5800 m (8200–19,000 ft).

During mission 21 (late afternoon, local time), all aircraft profiles were dryer and exhibited a well-defined subsidence inversion whose base ranged from 1800 to 2500 m (6000–8200 ft). The August 4 Bethel rawinsonde at 0000 UTC (Figure 35) shows a deep stable layer between 700 and 800 mbar, which marked the lowest level to which subsidence had occurred

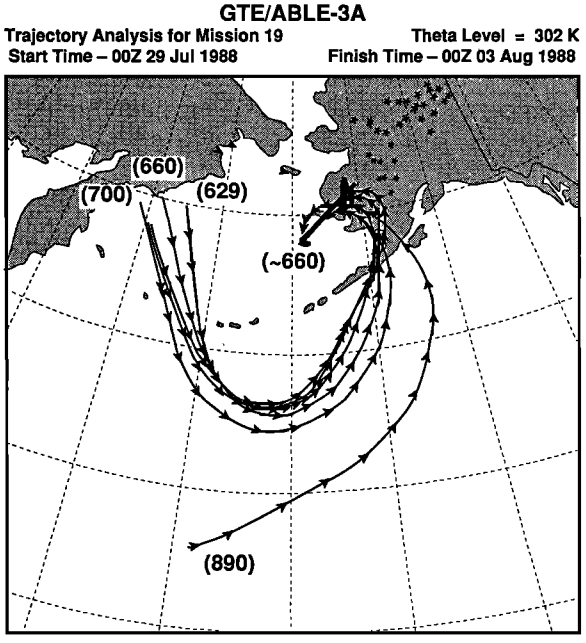

Fig. 31. The 302 K trajectory paths (5-day) for air arriving along the flight path during mission 19. Trajectory start time is 0000 UTC on July 29, 1988; trajectory end time is 0000 UTC on August 3, 1988.

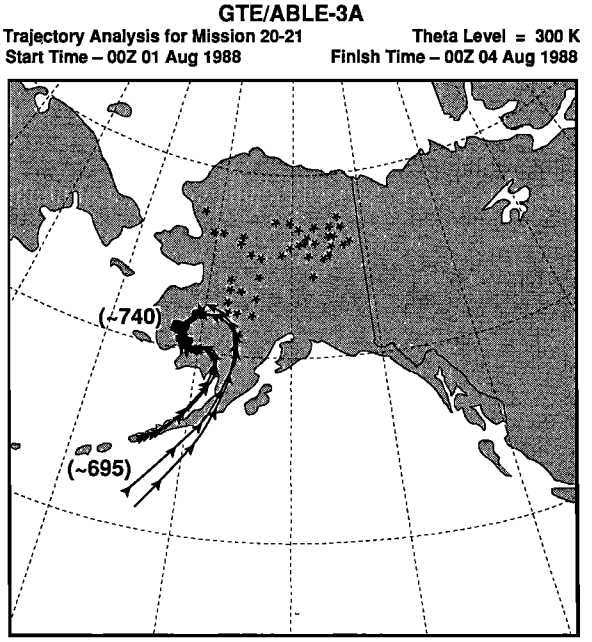

Fig. 33. The 300 K trajectory paths for air arriving along the flight path during missions 20 and 21. Trajectory start time is 0000 UTC on August 1, 1988; trajectory end time is 0000 UTC on August 4, 1988.

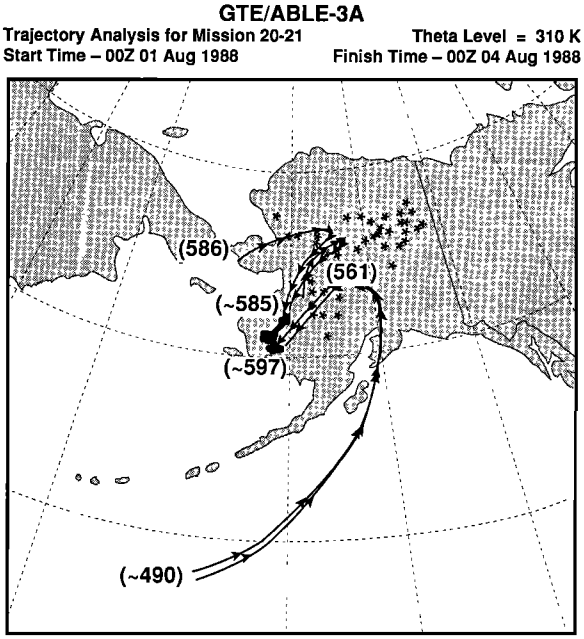

Fig. 34. The 310 K trajectory paths for air arriving along the flight path during missions 20 and 21. Trajectory start time is 0000 UTC on August 1, 1988; trajectory end time is 0000 UTC on August 4, 1988.

during the day. As before, multiple inversions were noted at higher altitudes, this time between 3300 and 5500 m (10,800–18,000 ft).

Trajectories at 300 and 310 K (Figures 33 and 34) suggest that smoke from fires burning to the northeast and east of Bethel was likely to have been advected toward the flight area. Airborne lidar (not shown) did detect enhanced aerosol plumes with positive ozone correlation between 3500 and 4200 m (11,500–13,800 ft).

Missions 22 and 23: August 7–8, 1988, Bethel, Alaska, to Cold Bay, Alaska, and North Pacific spirals, south of Cold Bay, Alaska. A weak low existed in the northern Gulf of Alaska which had been migrating eastward across the Bering Sea during the previous few days (Figure 4*r*). A polar vortex had been intensifying off the northern Siberian coast and was beginning to set up a northwesterly flow across the Bering Sea.

At lower levels (Figure 36 for mission 22, Figure 37 for mission 23), trajectories depict a north-northwestward transport of mP air ahead of the Bering Sea low, followed by a southeastward transport behind the low as it moved into the Gulf of Alaska. Trajectories originating over the southern Bering Sea looped over the Bethel region, while those originating in the northern Bering Sea passed over Siberia before moving toward the flight region. Since this low-level mP air was shown to have spent some time over either

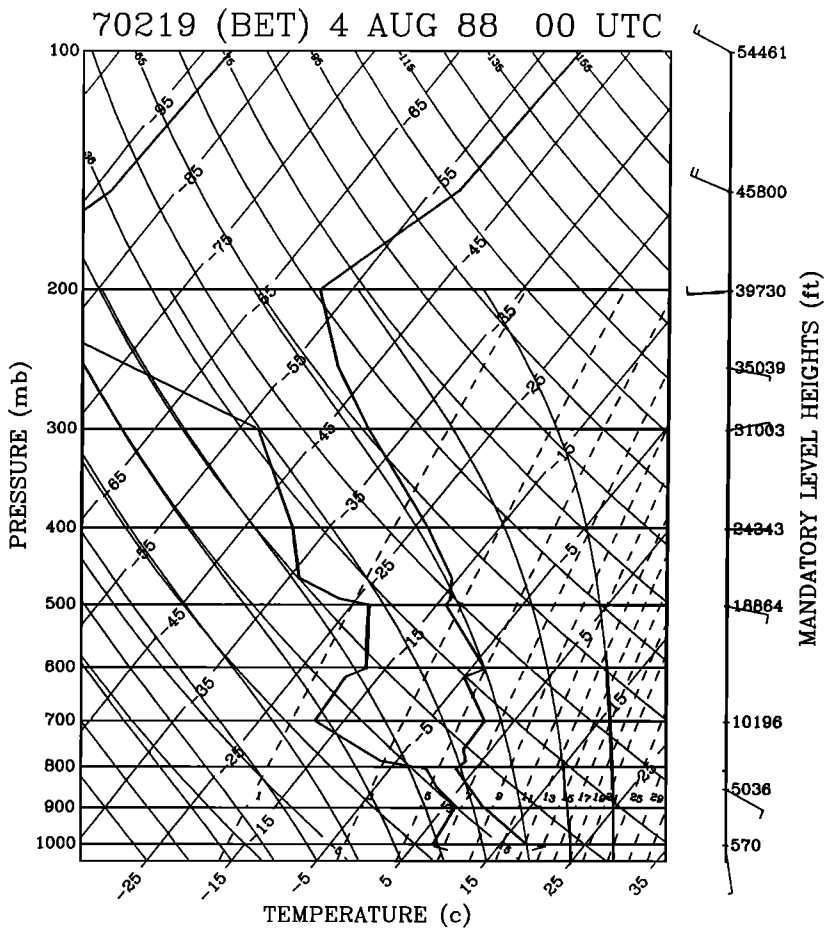

Fig. 35. The Bethel, Alaska rawinsonde at 0000 UTC on August 4, 1988, plotted on a Skew-*t*/log-*p* thermodynamic diagram. Dew point is plotted to the left of the temperature.

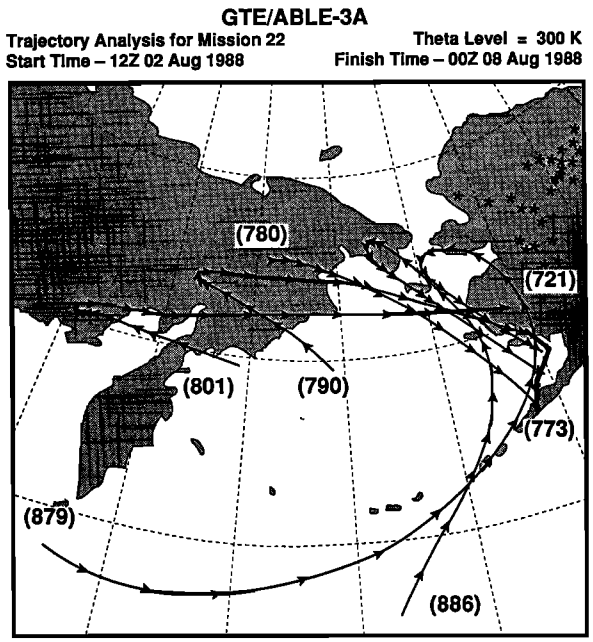

Fig. 36. The 300 K trajectory paths (5.5-day) for air arriving along the flight path during mission 22. Trajectory start time is 1200 UTC on August 2, 1988; trajectory end time is 0000 UTC on August 8, 1988.

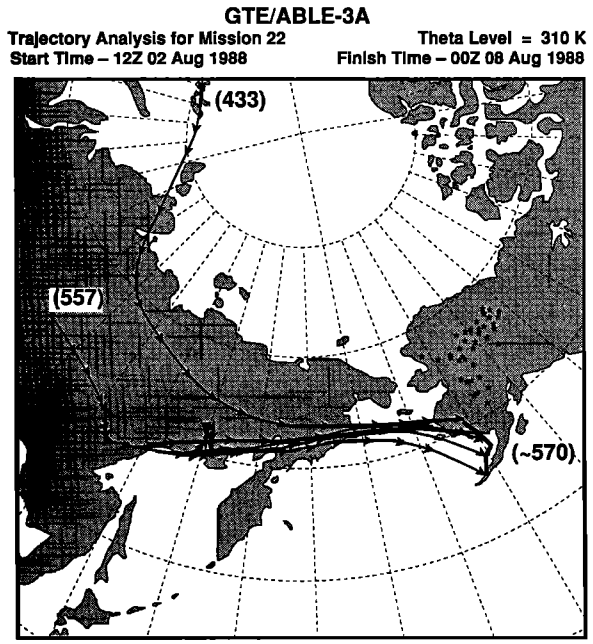

Fig. 38. The 310 K trajectory paths (5.5-day) for air arriving along the flight path during mission 22. Trajectory start time is 1200 UTC August 2, 1988; trajectory end time is 0000 UTC on August 8, 1988.

Alaska or Siberia, some fire smoke or industrial pollution (e.g., coal fields in Siberia) could have been acquired. Trajectories at higher altitudes (Figure 38 for mission 22, Figure 39 for mission 23) generally showed cP air moving eastward across Siberia, then southeastward across the Bering Sea. However, one trajectory along the 310 K surface for mission 23 (Figure 39) was shown to have come from interior Alaska, where extensive fires were still burning.

Satellite imagery depicted extensive low stratus over the Bering Sea, with one small clear area over Bristol Bay where the aircraft did its first mission 22 spiral. During mission 23, an elongated clear area developed along the leeward side of the Alaska Peninsula and the Aleutian Islands as the mountains and island volcanoes blocked the northwest-to-southeast flow of shallow marine layer stratus.

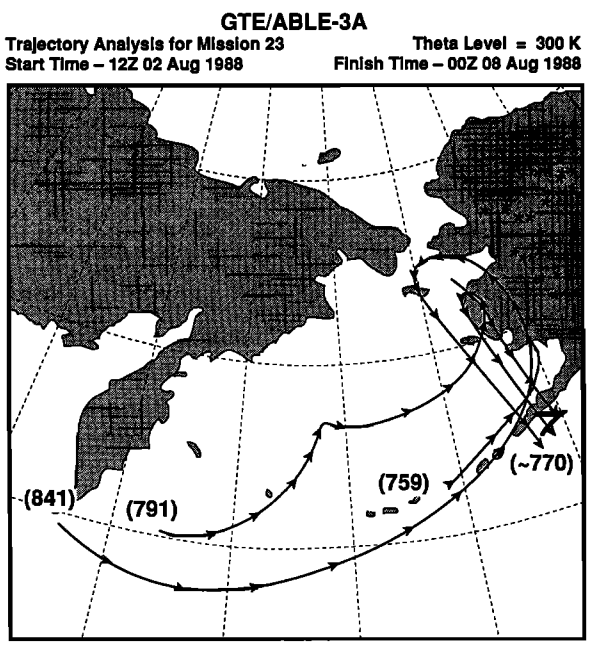

Fig. 37. The 300 K trajectory paths (5.5-day) for air arriving along the flight path during mission 23. Trajectory start time is 1200 UTC on August 2, 1988; trajectory end time is 0000 UTC on August 8, 1988.

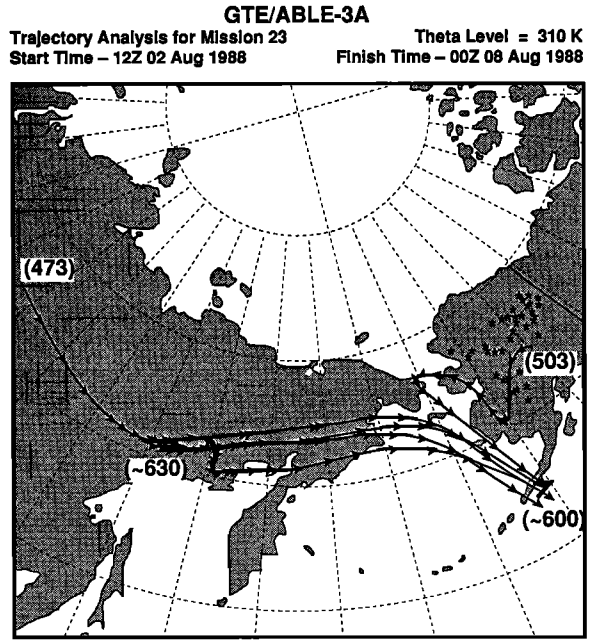

Fig. 39. The 310 K trajectory paths (5.5-day) for air arriving along the flight path during mission 23. Trajectory start time is 1200 UTC on August 2, 1988; trajectory end time is 0000 UTC on August 8, 1988.

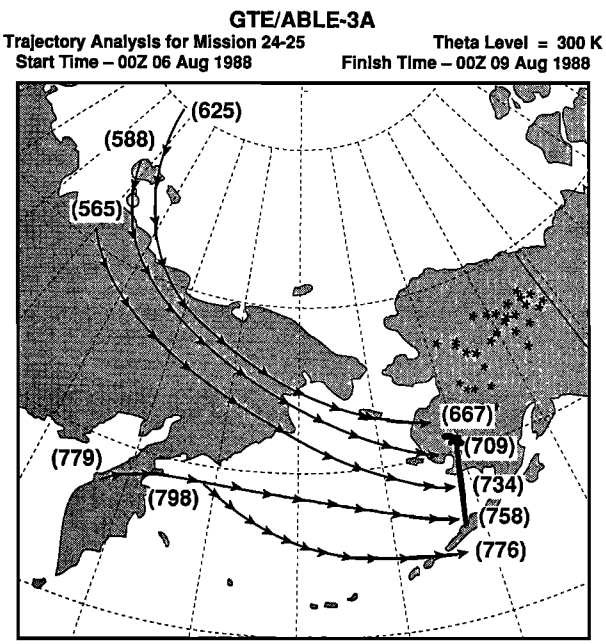

Fig. 40. The 300 K trajectory paths for air arriving along the flight path during missions 24 and 25. Trajectory start time is 0000 UTC on August 6, 1988; trajectory end time is 0000 UTC on August 9, 1988.

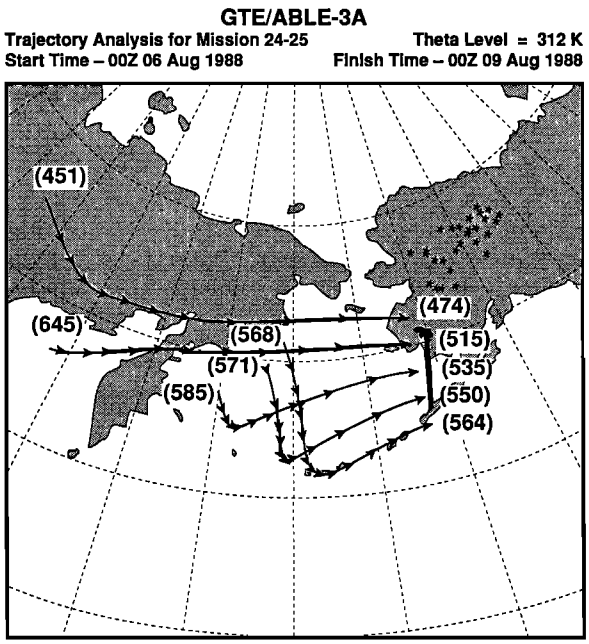

Fig. 41. The 312 K trajectory paths for air arriving along the flight path during missions 24 and 25. Trajectory start time is 0000 UTC on August 6, 1988; trajectory end time is 0000 UTC on August 9, 1988.

Missions 24 and 25: August 8–9, 1988, Cold Bay, Alaska to Bethel, Alaska, and land-sea interface, south of Bethel, Alaska. The strong polar vortex off the northern Siberian coast continued to generate a westerly flow across the Bering Sea (Figure 4*s*). A very dry and stable middle troposphere was depicted by Bethel rawinsonde reports, and temperature profiles during aircraft spirals showed a strong subsidence layer temperature inversion capping the marine layer over the eastern Bering Sea.

Trajectories at all levels depict a general west-to-east transport of cP air from Siberia toward the immediate Bethel area, and a westerly flow of modified cP air across the Bering Sea toward Bristol Bay (Figures 40 and 41).

During the northbound flight of mission 24, the aircraft flew at 3000 m (θ = 300 K, Figure 40) and at 4500 m (θ = 310 K, Figure 41). The air sampled at the lower altitude was driest, which can be explained by examining trajectories along the 300 K and 310 K surfaces. The 300 K trajectories originated farther north over northern Siberia, where moisture was less abundant, and these air parcels experienced stronger subsidence than those at the higher altitude. Aircraft spirals during mission 25 again revealed the dry middle troposphere over the Bering Sea that was noted on mission 24.

Mission 26: August 9–10, 1988, flux flight 3, near Bethel, Alaska. The polar vortex remained stationary over the Arctic Ocean north of Siberia (Figure 4*t*). Another low was developing over the Bering Sea and advecting significant moisture at all levels toward the Bethel area. Low-level trajectories (Figure 42) indicate that the polar vortex had been transporting cP air southeastward towards Bethel during the previous three days. This cP air begins to show a northward retreat 12–24 hours prior to the mission, signalling the approach of the Bering Sea low and its moist southerly flow of mP air.

Cross sections and Bethel rawinsondes (not shown) indicated that the leading edge of the moist southwesterly flow of mP air was first becoming evident in the middle troposphere during the day. The aircraft remained low enough to have sampled the shallow, drier cP air mass that was being overrun by the advancing moisture-laden mP air.

Mission 27: August 11–12, 1988, Bethel, Alaska, to Barrow, Alaska. The polar vortex which had been intensifying

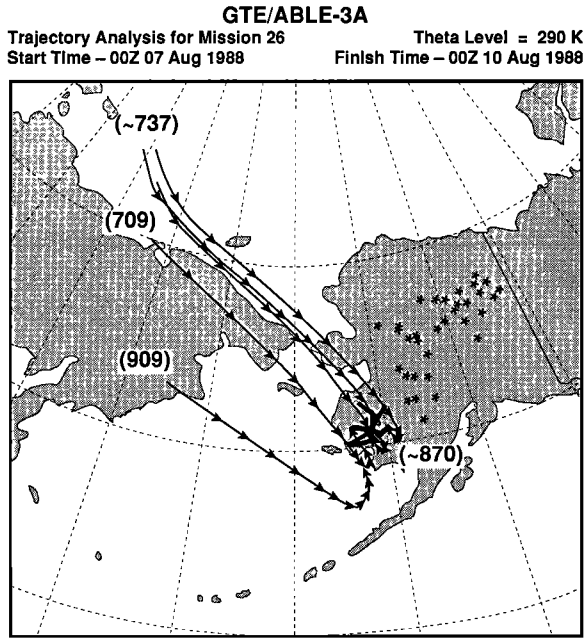

Fig. 42. The 290 K trajectory paths for air arriving along the flight path during mission 26. Trajectory start time is 0000 UTC on August 7, 1988; trajectory end time is 0000 UTC on August 10, 1988.

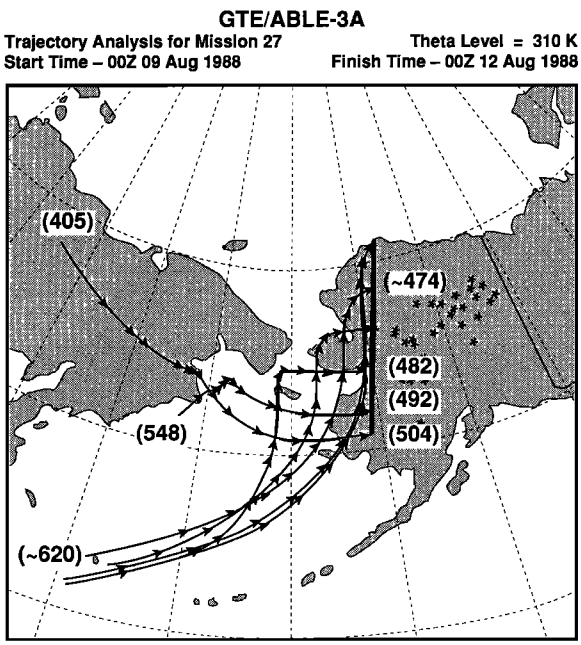

Fig. 43. The 310 K trajectory paths for air arriving along the flight path during mission 27. Trajectory start time is 0000 UTC on August 9, 1988; trajectory end time is 0000 UTC on August 12, 1988.

over the Arctic Ocean north of Siberia since early August was now quite strong and extensive in areal coverage (Figure 4*u*). A short-wave trough rotating around this polar vortex had phased with the Bering Sea low and moved into western Alaska, bringing abundant moisture across the flight region. Trajectories arriving in the vicinity of Bethel indicate that cP air had been transported east-southeastward across northern Siberia and the northern Bering Sea (Figure 43). Along the remainder of the flight track, mP air had been transported northeastward as the Bering Sea low migrated toward Barrow.

Cross sections (not shown) showed a dry area aloft over Bethel, then extensive moisture in the lower and middle troposphere for the remainder of the flight path, reflected by the saturated air which was sampled by the aircraft. "Stratospheric threshold" potential vorticity values analyzed at altitudes near that of the aircraft suggest that stratosphere/troposphere exchange had been occurring behind the Bering Sea low as it approached Barrow.

Mission 28: August 12, 1988, Barrow, Alaska, to Thule, Greenland. A polar vortex had been stationary over Baffin Island during the previous week, while a weakening area of low pressure had moved from the Bering Sea to the Arctic Ocean north of Barter Island, Alaska (Figure 4*v*). Between these two lows, a weak elongated north-to-south ridge of high pressure was located over the Queen Elizabeth Islands of northern Canada. Trajectories (Figure 44) show an eastward transport of cP air from the north Siberian coast toward the Barrow region, while air over the Arctic Ocean had moved north-northeastward across Alaska. Over the Queen Elizabeth Islands, a weak and erratic flow was evident within the ridge of high pressure. Finally, trajectories revealed a counterclockwise transport around the Baffin Island low toward the Thule region.

The aircraft sampled moist air associated with the area of low pressure over the Arctic Ocean. One exception was noted between 1854 and 1920 UTC, northeast of Barter Island, Alaska, where dew points dropped from −20°C to near −50°C. This dry pocket of air was likely associated with a very localized stratospheric intrusion near the core of the Arctic Ocean low, as lidar (not shown) revealed enhanced ozone structure working its way down to near 7 km. This low was clearly depicted on polar orbiter satellite imagery, and resembles the Arctic-front type of polar low which forms or intensifies along differential heating boundaries where ice pack lies adjacent to warmer open water [*Twitchell et al.*, 1989].

As the aircraft approached Thule, lower dew points were measured, and trajectories indicated the air at that location had been transported from a different region than that which was sampled over the Queen Elizabeth Islands.

Mission 29: August 13, 1988, polar flight, northeast of Thule, Greenland. The persistent polar vortex remained stationary over Baffin Island. The weak elongated area of high pressure which had been over the Queen Elizabeth Islands was building into northern Greenland. At levels near the maximum aircraft altitude, trajectories in the vicinity of Thule show that cP air had been transported counterclockwise around the Baffin Island low from eastern Canada, while cP air that was north of Alert had remained nearly stationary over the northern Queen Elizabeth Islands (Figure 45). Near the surface, trajectories in the Thule region indicate a northward transport across Greenland, while air north of Alert had been moving slowly southeastward across the Arctic Ocean icepack (Figure 46).

The aircraft encountered cold dry air at all altitudes, except at 150 m over the ice pack where the air was saturated. From 1719 to 1742 UTC, very dry air (dew points below −40°C) was sampled between 4600 m and 5600 m (15,200–18,500 ft). This very dry layer could have contained aged stratospheric air, judging from the high values of

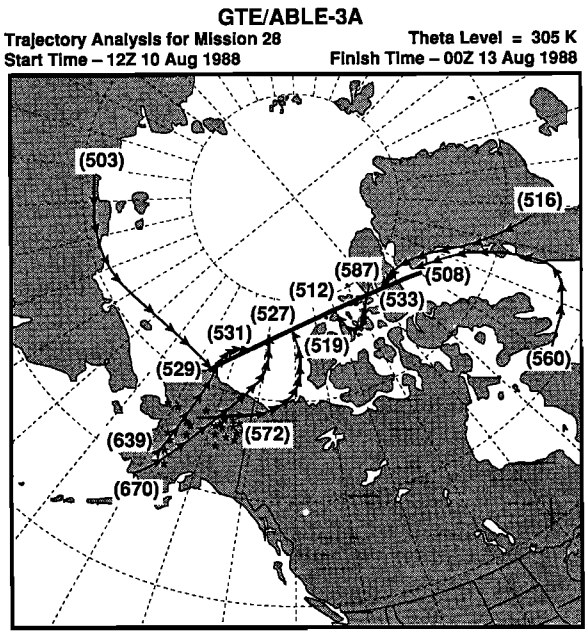

Fig. 44. The 305 K trajectory paths for air arriving along the flight path during mission 28. Trajectory start time is 1200 UTC on August 10, 1988; trajectory end time is 0000 UTC on August 13, 1988.

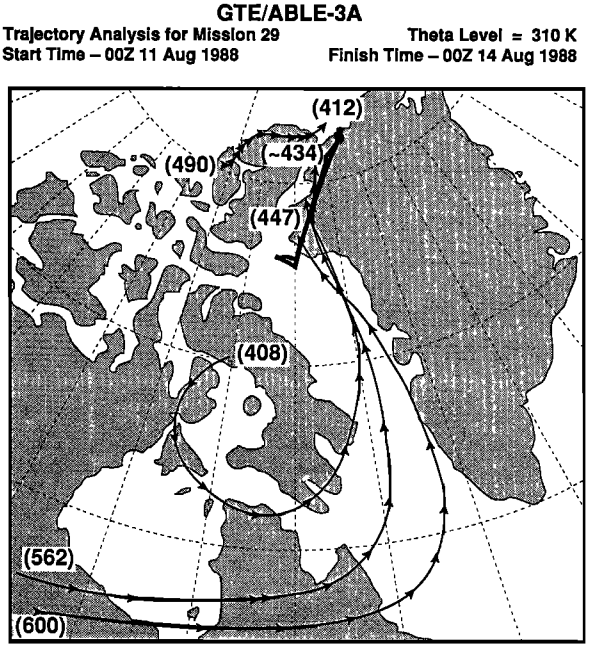

Fig. 45. The 310 K trajectory paths for air arriving along the flight path during mission 29. Trajectory start time is 0000 UTC on August 11, 1988; trajectory end time is 0000 UTC on August 14, 1988.

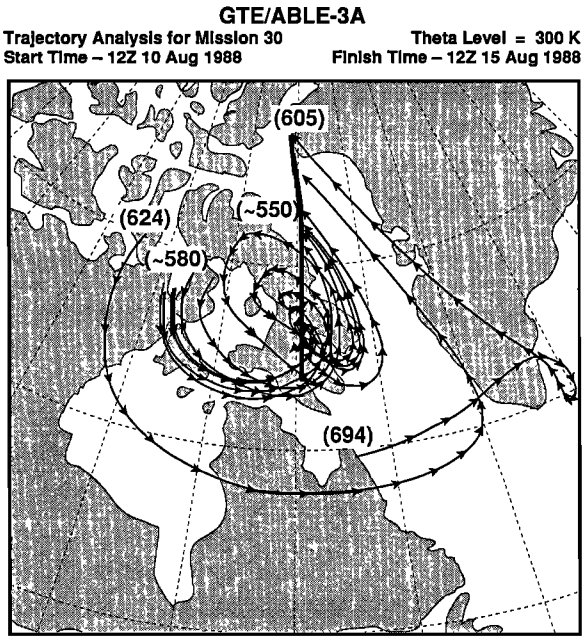

Fig. 47. The 300 K trajectory paths (5-day) for air arriving along the flight path during mission 30. Trajectory start time is 1200 UTC on August 10, 1988; trajectory end time is 1200 UTC on August 15, 1988.

potential vorticity which were analyzed around the fringes of the Baffin Island low (and also around the more intense polar vortex which had been situated over northern Siberia since early August).

Missions 30 and 31: August 15, 1988, Thule, Greenland, to Frobisher Bay, Northwest Territories, and Frobisher Bay to Goose Bay, Labrador. The major synoptic feature that affected mission 30 was the low that had been stationary over Baffin Island during the previous week. The westerly flow in association with the polar jet stream across central Canada was the main synoptic feature affecting mission 31. Trajectories for mission 30 (Figure 47) show the counterclockwise transport of cP air around the Baffin Island low. The air that was sampled at the beginning of the flight (over Thule) had been transported eastward from eastern Canada, then northward across Greenland, while air sampled for the remainder of the mission had generally been confined to the tight circulation within the Baffin Island low. Trajectories for mission 31 (Figure 48) depict a strong west-to-east transport across northern Canada.

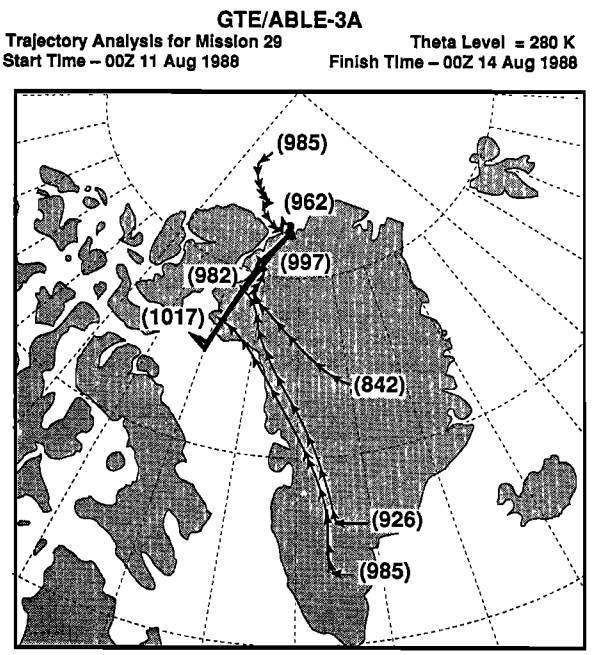

Fig. 46. The 280 K trajectory paths for air arriving along the flight path during mission 29. Trajectory start time is 0000 UTC on August 11, 1988; trajectory end time is 0000 UTC on August 14, 1988.

During mission 30, the high-altitude portion of the flight was generally dry with dew points between −30 and −40°C. Higher dew points were measured as the plane approached the Baffin Island low. Airborne lidar (not shown) depicted the tropopause lowering upon approach of the low, and a well-defined stratospheric intrusion was evident as an enhancement in the ozone distribution down to altitudes near 7 km (Plate 3). Additionally, values of potential vorticity greater than the "stratospheric threshold" were analyzed in that region.

Dew points measured on mission 31 were slightly higher as the aircraft encountered increased moisture associated with a weak wave embedded in the polar jet stream. Cross sections (not shown) revealed the marked increase in midtropospheric moisture along the more southerly flight track of mission 31.

Mission 32: August 16, 1988, Goose Bay, Labrador, to Portland, Maine. An elongated area of low pressure existed over the Gulf of St. Lawrence and the surrounding Canadian Maritime Provinces. As this low weakened and became less defined, a trough of low pressure over Hudson Bay moved southeastward to the New England coast. Tra-

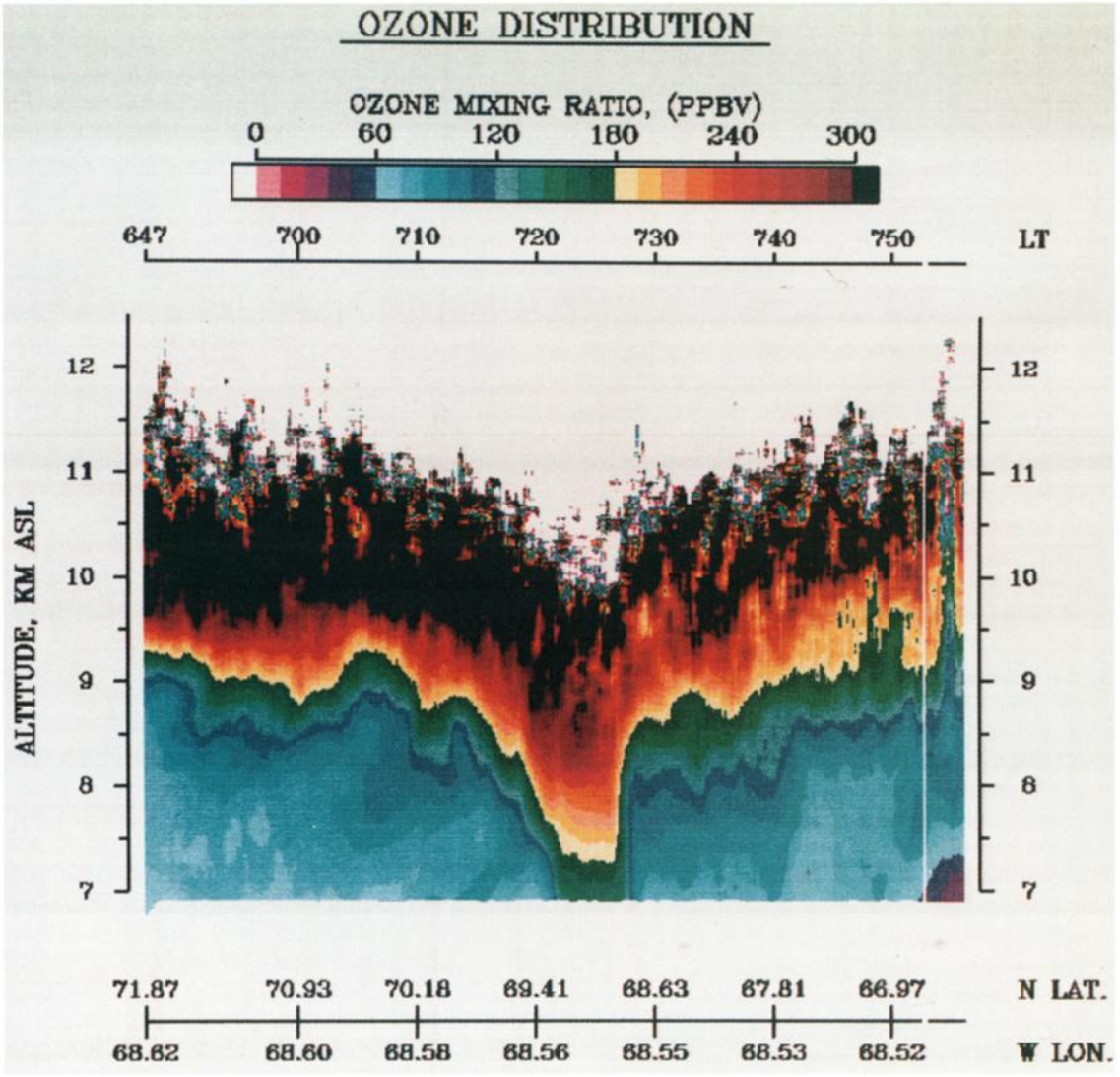

Plate 3. Airborne lidar measurements of ozone mixing ratio (ppbv) in the vicinity of the Baffin Island low during mission 30 on August 15, 1988. Times (LT) displayed along the top of the panel are Alaskan Daylight Time (UTC − 8 hours). A well-defined stratospheric intrusion was responsible for enhanced ozone concentrations down to altitudes near 7 km.

jectories (Figure 49) indicate that modified continental air transported counterclockwise around the Maritime Provinces low was sampled for the first portion of the flight. As the aircraft neared New Brunswick and Maine, a transition into continental air which had been moving northeastward from the central United States or southeastward from central Canada was evident.

The aircraft sampled relatively dry air (dew points between −20°C and −30°C) at 5 km over Newfoundland and Quebec. A cross section along the flight path (not shown) revealed a significant increase in moisture at all levels over New England, which was reflected by the higher dew points (−5°C to −10°C) measured over that region.

Mission 33: August 17, 1988, Portland, Maine, to Langley Research Center, Hampton, Virginia. The trough of low pressure that was affecting mission 32 was exiting the New England coast. In addition, a ridge of high pressure was centered over the central and eastern United States.

Trajectories (Figure 50) indicate a clockwise transport of continental air around the ridge of high pressure. The northerly flow of air sampled during the first (high-altitude) portion of the flight had been moving eastward across southern Canada behind the trough. Toward the end of the flight leg, including the spiral down over Wallops Island, Virginia, transport from the central United States was evident at all altitudes.

The aircraft sampled dry air (dew points between −20°C and −35°C) off the New England coast behind the exiting trough. An area of potential vorticity near the stratospheric threshold was evident in the wake of the trough, suggesting stratosphere/troposphere exchange was taking place as low as the maximum flight altitude (5 km). Airborne lidar (not shown) depicted enhanced aerosol scattering in the lowest 1–2 km of the troposphere off the eastern seaboard from Massachusetts to Virginia, a signature of the hazy air mass which had been resident over the continental United States.

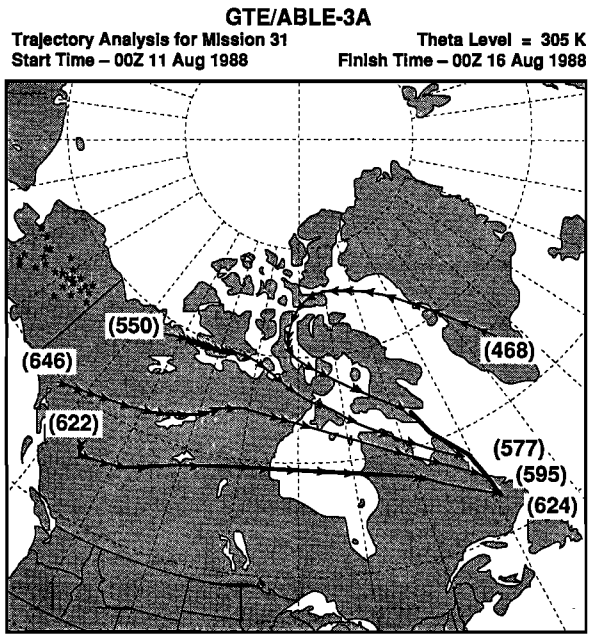

Fig. 48. The 305 K trajectory paths (5-day) for air arriving along the flight path during mission 31. Trajectory start time is 0000 UTC on August 11, 1988; trajectory end time is 0000 UTC on August 16, 1988.

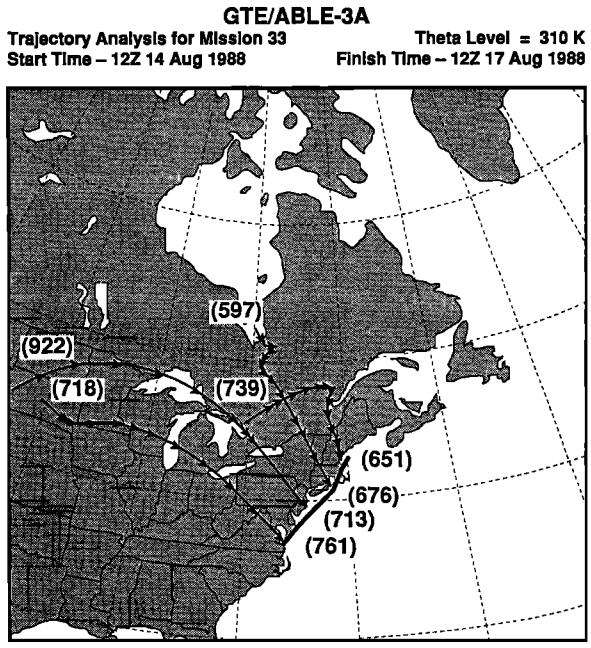

Fig. 50. The 310 K trajectory paths for air arriving along the flight path during mission 33. Trajectory start time is 1200 UTC on August 14, 1988; trajectory end time is 1200 UTC on August 17, 1988.

SUMMARY

Isentropic back trajectories calculated for the ABLE 3A flight series indicate that Siberia and the northern Pacific Ocean were the two most likely source areas for long-range (400–3000 km) atmospheric transport to the Alaskan study regions during July and August 1988 (Figures 51 and 52). Transport to the Barrow region was frequently influenced by polar vortices and associated short-wave troughs of low pressure over the Arctic Ocean, while the Bethel area was most often affected by lows migrating across the Bering Sea and the Gulf of Alaska, as well as ridges of high pressure which built into interior Alaska.

Table 2 groups the Alaskan flights into their corresponding

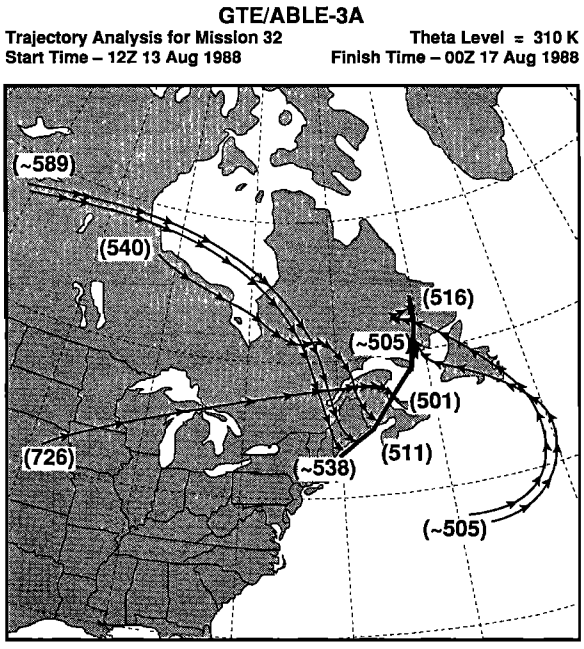

Fig. 49. The 310 K trajectory paths for air arriving along the flight path during mission 32. Trajectory start time is 1200 UTC on August 13, 1988; trajectory end time is 0000 UTC on August 17, 1988.

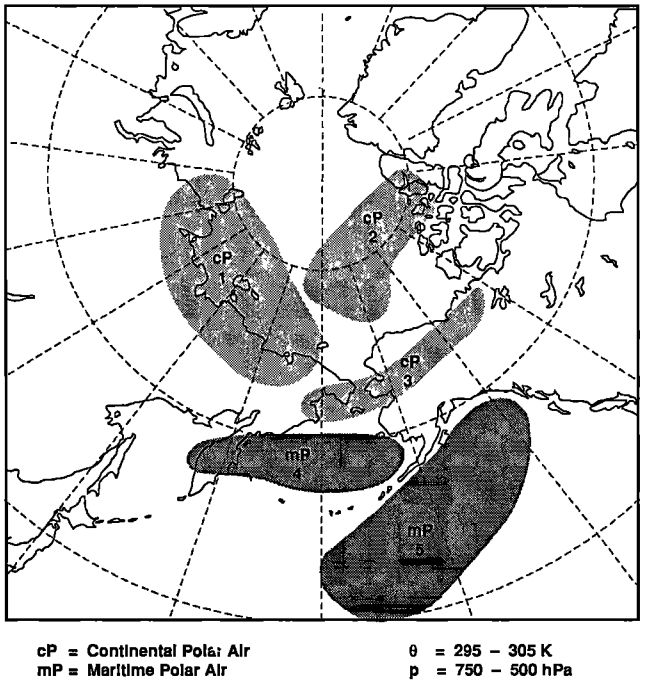

Fig. 51. Low-level (295–305 K, 500–750 hPa) air mass source areas for 3-day transport to the Alaskan study regions. Air mass classifications (cP, continental polar; mP, maritime polar) are also indicated.

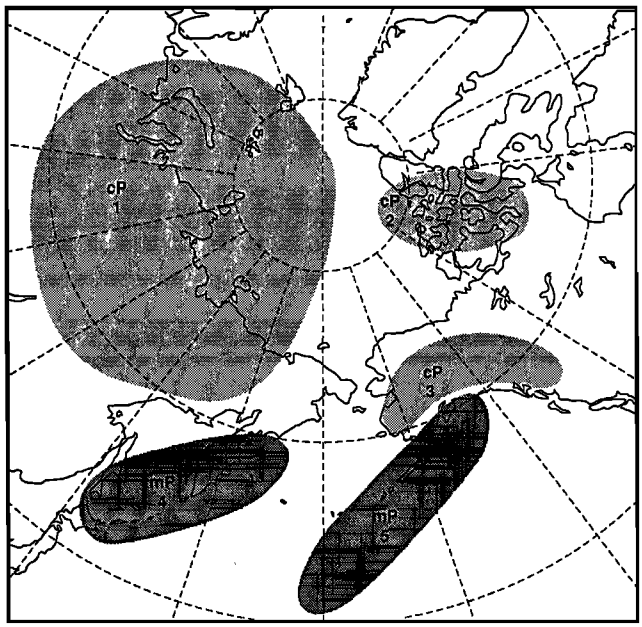

Fig. 52. High-level (310–320 K, 300–500 hPa) air mass source areas for 3-day transport to the Alaskan study regions. Air mass classifications (cP, continental polar; mP, maritime polar) are also indicated.

five principal source areas found in Figures 51 and 52, at low levels and at high levels. It can be seen that for the low levels (below 500 hPa) the flights are about evenly divided between the three cP source areas (1, 2, and 3) and the two mP source areas (4 and 5). At high levels (above 500 hPa) a definite bias toward the three cP source areas is evident.

Smoothing out the daily synoptic-scale features to reveal the larger scale mean atmospheric circulation showed that a

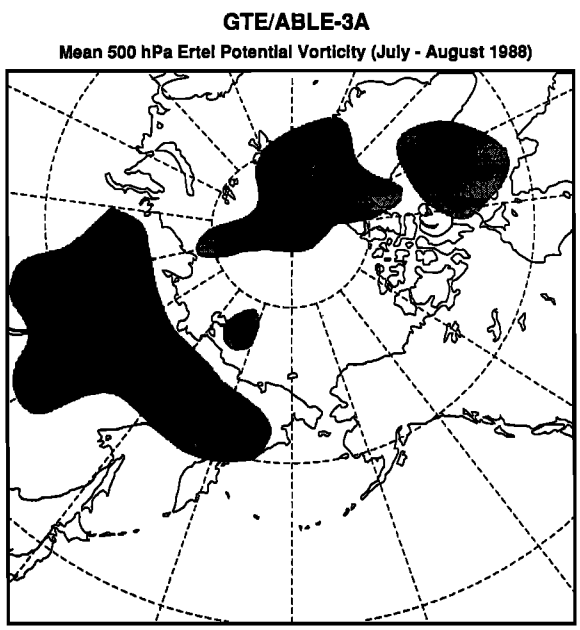

Fig. 53. Mean Ertel potential vorticity exceeding 7×10^{-5} K m^2 kg^{-1} s^{-1}, averaged over the July–August 1988 time period along the 500-hPa surface.

TABLE 2. Alaskan Flights Grouped With Their Corresponding Five Air Mass Source Areas (See Figures 51 and 52)

Source Area	Air Mass	Missions
	Low-Level (Theta 1= 295–305 K, p = 750–500 hPa)	
1	*cP*	9, 10, 11, 13, 24, 25, 26
2	*cP*	12, 13
3	*cP*	6, 26
4	*mP*	14, 15, 22, 23, 24, [illegible]
5	*mP*	16, 18, 19, 20, 21, 22
	High-Level (Theta = 310–320 K, p = 500–300 hPa)	
1	*cP*	7, 8, 9, 10, 11, 12, 13, 14, 15, 20, 21, 22, 23, 27
2	*cP*	12
3	*cP*	5, 6, 7, 20, 21, 23
4	*mP*	19
5	*mP*	17, 19, 20, 21, 27

Air mass classifications are cP, contimental polar; mP, marine polar.

ridge of high pressure was dominant over Alaska during July 1988. That month was warmer and dryer than normal over much of the study region, with Bethel recording a mean temperature 2.9°C above normal and precipitation 26% of the normal amount for the month. As a result, the 1988 Alaska fire season was the most active of the past decade, with over 600 fires and more than 8500 km^2 burned statewide.

Airborne lidar measurements verified the presence of biomass burning plumes trapped in thin subsidence layer temperature inversions, most notably on missions 4, 13, 14, and 21. It is likely that most of the burning plumes encountered originated from the abundant Alaskan fires, but some long-range transport of smoke from Siberian fires was evident.

Several cases of stratosphere/troposphere exchange were noted, based upon potential vorticity analyses and aircraft lidar data, especially in the Barrow region (missions 7, 8, 9, 13, and 27) and during transit flights to and from Alaska (missions 2, 3, 4, 28, 29, and 30). Region 1 (Figures 51 and 52, Table 2) was the source area for all of these stratospheric cases. Figure 53 shows that this was also a region of high mean potential vorticity, as averaged over the July–August 1988 period at the 500 hPa surface (the mid-troposphere). It appears that region 1 was a favored area for stratospheric input to the troposphere; this stratospheric air was then frequently transported toward the ABLE 3A study region.

Further investigations of the meteorology affecting Alaska and the Arctic regions of North America will focus on more detailed cross-sectional analyses of potential vorticity to determine the magnitude of the influence of the stratosphere on the such parameters as the ozone and aerosol budgets in the summer Arctic troposphere. In addition, longer back trajectories (1–2 weeks) could be utilized in conjunction with polar-orbiter advanced very high resolution radiometer satellite imagery over the Soviet Union to study the impact of long-range atmospheric transport of biomass burning plumes on the ABLE 3A study regions. Even though analysis uncertainties and model simplifications would limit the accuracy of individual 1–2 week back trajectories, it is felt that a large number of such calculations during many summer

seasons could yield a reasonable representation of the general Arctic transport.

Acknowledgments. The authors would like to express their appreciation to Phil Haagensen for providing the original trajectory code, to Sandra Barnes for the extensive art work, and to the National Weather Service personnel in Anchorage, Alaska, for hosting the GTE meteorological team and equipment.

REFERENCES

Alaska Fire Service, 1988 Alaska Fire Service fire season statistics, U.S. Dep. of Interior/Bur. of Land Manage., Fairbanks, 1989.

Bakwin, P. S., S. C. Wofsy, S. Fan, and D. R. Fitzjarrald, Measurements of NO_x and NO_y concentrations and fluxes over Arctic tundra, *J. Geophys. Res.*, this issue.

Barrie, L. A., R. M. Hoff, and S. M. Daggupaty, The influence of mid-latitudinal pollution sources on haze in the Canadian Arctic, *Atmos. Environ.*, *15*, 1407–1419, 1981.

Bergeron, T., Über die dreidimensional verknüpfende wetteranalyse, *Geofys. Publikasjoner*, *5*(6), 1928.

Blake, D. R., D. F. Hurst, T. W. Smith, Jr., W. J. Whipple, T. Y. Chen, N. J. Blake, and F. S. Rowland, Summertime measurements of selected nonmethane hydrocarbons in the Arctic and sub-Arctic during the 1988 Arctic Boundary Layer Expedition (ABLE 3A), *J. Geophys. Res.*, this issue.

Borys, R. D., and K. A. Rahn, Long-range atmospheric transport of cloud-active aerosol to Iceland, *Atmos. Environ.*, *15*, 1491–1501, 1981.

Browell, E. V., C. F. Butler, S. A. Kooi, M. A. Fenn, R. C. Harriss, and G. L. Gregory, Large-scale variability of ozone and aerosols in the summertime Arctic and sub-Arctic troposphere, *J. Geophys. Res.*, this issue.

Danielsen, E. F., Trajectories: Isobaric, isentropic and actual, *J. Meteorol.*, *18*, 479–486, 1961.

Danielsen, E. F., Research in four-dimensional diagnosis of cyclonic storm cloud systems, *Rep. 66-30*, pp. 1–34, Air Force Cambridge Res. Lab., Bedford, Mass., 1966. (Available as *NTIS AD 670 847* from Natl. Tech. Inf. Serv., Springfield, Va.)

Gregory, G. L., B. E. Anderson, L. S. Warren, E. V. Browell, D. R. Bagwell, and C. H. Hudgins, Tropospheric ozone and aerosol observations: The Alaskan Arctic, *J. Geophys. Res.*, this issue.

Haagensen, P. L., and M. A. Shapiro, Isentropic trajectories for derivation of objectively analyzed meteorological parameters, *Tech. Note NCAR/TN-149*, 30 pp., Natl. Cent. for Atmos. Res., Boulder, Colo., 1979.

Harris, J. M., and J. D. Kahl, A descriptive atmospheric transport climatology for the Mauna Loa Observatory, using clustered trajectories, *J. Geophys. Res.*, *95*, 13,651–13,667, 1990.

Harriss, R. C., et al., The Arctic Boundary Layer Expedition (ABLE 3A): July–August 1988, *J. Geophys. Res.*, this issue.

Hoskins, B. J., M. E. McIntyre, and A. W. Robertson, On the use and significance of isentropic potential vorticity maps, *Q. J. R. Meteorol. Soc.*, *111*, 877–946, 1985.

Kahl, J. D., J. M. Harris, G. A. Herbert, and M. P. Olson, Intercomparison of three long-range trajectory models applied to Arctic haze, *Tellus*, *41B*, 524–536, 1989.

Miller, J. M., A five-year climatology of five-day back trajectories from Barrow, Alaska, *Atmos. Environ.*, *15*, 1401–1405, 1981.

Moore, J. T., Isentropic analysis and interpretation: Operational applications to synoptic and mesoscale forecast problems, *Rep. TN-87/002*, 85 pp., Air Weather Service (MAC), Scott Air Force Base, Ill., 1987.

Raatz, W. E., Tropospheric circulation patterns during the Arctic Gas and Aerosol Sampling Program (AGASP), March/April 1983, *Geophys. Res. Lett.*, *11*, 449–452, 1984.

Radke, L. F., P. V. Hobbs, and I. H. Bailey, Airborne observations of Arctic aerosols, 3, Origins and effects of air masses, *Geophys. Res. Lett.*, *11*, 401–404, 1984.

Rahn, K. A., Relative importance of North America and Eurasia as sources of Arctic aerosol, *Atmos. Environ.*, *15*, 1447–1455, 1981.

Sandholm, S. T., et al., Summertime tropospheric observations related to N_xO_y distributions and partitioning over Alaska: Arctic Boundary Layer Expedition 3A, *J. Geophys. Res.*, this issue.

Schnell, R. C., Arctic haze and the Arctic Gas and Aerosol Sampling Program (AGASP), *Geophys. Res. Lett.*, *11*, 361–364, 1984.

Shapiro, M. A., T. Hampel, and A. J. Krueger, The Arctic tropopause fold, *Mon. Weather Rev.*, *115*, 444–454, 1987.

Talbot, R. W., A. S. Vijgen, and R. C. Harriss, Soluble species in the Arctic summer troposphere: Acidic gases, aerosols, and precipitation, *J. Geophys. Res.*, this issue.

Taylor, G. F., *Elementary Meteorology*, 364 pp., Prentice-Hall, Englewood Cliffs, N. J., 1954.

Twitchell, P. F., E. A. Rasmussen, and K. L. Davidson (Eds.), *Polar and Arctic Lows*, 421 pp., A. Deepak, Hampton, Va., 1989.

A. S. Bachmeier, Lockheed Engineering and Sciences Company, Hampton, VA 23666.

E. V. Browell, D. R. Cahoon, Jr., and M. C. Shipham, Atmospheric Sciences Division, NASA Langley Research Center, Hampton, VA 23665.

(Received March 27, 1991;
revised September 13, 1991;
accepted October 15, 1991.)